Dynamic Learning-Based Optimal Sliding Mode Control for Fuzzy Singularly Perturbed Systems With FDI Attacks and Communication Constraints

Yan Li, Ding Zhu, Lijuan Zha, Jinliang Liu, *Senior Member, IEEE*, and Engang Tian, *Senior Member, IEEE*

***Abstract*—This article explores the sliding mode control (SMC) issue for Takagi–Sugeno (T–S) fuzzy model-based singularly perturbed systems (SPSs) with bandwidth-limited and cyberattack-threatened communication. First, to ease the communication constraints on system performance, a novel dynamic event-triggering mechanism (DETM) is designed to reduce the transmission of redundant data adaptively; moreover, considering that the network bandwidth is now generally divided into multiple channels, a multichannel-oriented weighted try-once-discard (MWTOD) protocol is proposed to realize collision-free data transmission over multiple communication channels at event-triggering instants. Then, focusing on false data injection (FDI) attacks, which are a type of commonly encountered security threat, a secure observer-assisted sliding mode controller with undetermined gain matrices is presented. Subsequently, by constructing an augmented T–S fuzzy SPS model, the sufficient conditions for the stability with guaranteed H_∞ performance of the system and the reachability of the sliding surface are analyzed, which is accompanied by the derivation of the observer and controller gains. To improve the control performance, a dynamic learning-based adaptive particle swarm optimization (APSO) algorithm is further devised with the aim to minimize the sliding domain. Simulations are finally conducted to verify the effectiveness of the proposed SMC strategy.**

***Index Terms*—Dynamic event-triggering mechanism (DETM), false data injection (FDI) attacks, fuzzy singularly perturbed systems (SPSs), multichannel-oriented weighted try-once-discard (MWTOD) protocol, sliding mode control (SMC).**

I. Introduction

NOWADAYS, with the continuous investigation on networked control systems (NCSs) [1], it is acknowledged that traditional models driven by one timescale are no longer adequate to depict some dynamic systems presented multitimescale feature, such as hypersonic vehicle systems [2], electronic circuit systems [3], and robot control systems [4]. In view of this, a singular perturbation parameter (SPP) ε is generally introduced to differentiate different timescales, and the systems are accordingly named as singularly perturbed systems (SPSs). Some explorations on the dynamic analysis of SPSs have been conducted in recent years. For instance, Wang et al. [5] focused on singularly perturbed switched systems with dwell-time switching laws, and designed a slow feedback control approach to analyze the extended dissipativity properties of the systems; the fault detection problem over SPSs with hidden Markov models and bandwidth-limited communication was studied in [6]. In addition to the discussed works concerned with linear SPSs, extensive research attentions have been attracted to the nonlinearities observed from SPSs.

Nonlinearities inevitably lead to difficulties in the design and analysis of control strategies for SPSs. An effective method to cope with the challenge is to utilize a Takagi–Sugeno (T–S) fuzzy model to relax the nonlinear constraint. By recurring to the T–S fuzzy model, the dynamics of nonlinear systems can be described by a set of linear subsystems grouped by membership functions. Given the powerful nonlinear approximation and uncertainty handling capabilities exhibited by the T–S fuzzy model, the research issues related to T–S fuzzy SPSs have been widely discussed. As an illustration, Cheng et al. [7] investigated static output feedback control of fuzzy Markovian switched SPSs with asynchronous quantized measurement outputs; for nonlinear SPSs under a nonperiodic multirate sampling scenario, a fuzzy parallel distributed compensation scheme was explored to handle control issues in [8].

Comparing with the aforementioned control methods, sliding mode control (SMC) presents more effectiveness in nonlinear control due to its fast response, excellent disturbance rejection, and strong robustness. As a variable structure control scheme, SMC can resist external disturbances and parameter uncertainties by constructing a sliding surface and adjusting corresponding parameters [9]. In the existing works, significant progress has been obtained in devising SMC schemes for fuzzy SPSs [10]. Additionally, given that system states are often unmeasurable in practice, it is more desirable to develop observer-based SMC strategies [11]. With regard to this, this article will focus on designing an SMC approach for T–S fuzzy SPSs based on constructing an appropriate observer.

Received 24 November 2025; accepted 13 January 2026. Date of publication 6 February 2026; date of current version 16 April 2026. This work was supported in part by the National Natural Science Foundation of China under Grant 62373252 and Grant 62273174, and in part by the Natural Science Foundation of Jiangsu Province of China under Grant BK20230063. This article was recommended by Associate Editor H. Li. *(Corresponding author: Jinliang Liu.)*

Yan Li and Ding Zhu are with the School of Computer and Artificial Intelligence, Nanjing University of Finance and Economics, Nanjing, Jiangsu 210023, China (e-mail: ylnjue@163.com; zd17312265983@163.com).

Lijuan Zha is with the College of Science, Nanjing Forestry University, Nanjing, Jiangsu 210037, China (e-mail: zhalijuan@vip.163.com).

Jinliang Liu is with the School of Computer Science, Nanjing University of Information Science and Technology, Nanjing, Jiangsu 210044, China (e-mail: liujinliang@vip.163.com).

Engang Tian is with the School of Optical-Electrical and Computer Engineering, University of Shanghai for Science and Technology, Shanghai 200093, China (e-mail: tianengang@163.com).

Color versions of one or more figures in this article are available at https://doi.org/10.1109/TSMC.2026.3655429.

Digital Object Identifier 10.1109/TSMC.2026.3655429

Considering that the network bandwidth is becoming limited with the increase of data volume in NCSs, the devise of the SMC approach will be seriously hindered. The available methods to deal with the communication constraints can be mainly categorized into two types, i.e., communication scheduling protocols and event-triggering mechanisms (ETMs). For the former, the data will be sent by their generators regardless of the bandwidth limitation of the network, and then, the information will be scheduled to be released into the network based on the predefined policy so as to avoid the data collision caused by the communication constraints. The typical scheduling protocols involve the round robin (RR) protocol, stochastic communication (SC) protocol, and weighted try-once-discard (WTOD) protocol. Differing from the first two classes of protocols, which did not consider the importance of the data to be scheduled, the WTOD protocol offers superiority to the most important data, and then better transmission performance can be expected [12]. Several studies on control problems over fuzzy SPSs under the WTOD protocol have been reported [13], [14]. However, the WTOD protocol adopted in these related works is based on single-channel communication, and thus cannot be applied to multichannel communication, where multiple candidates can be simultaneously scheduled via assigning a dedicated communication channel for each of them. Given that multichannel communication is now maturely enabled in both wired and wireless networks [15], [16], the multichannel-oriented WTOD (MWTOD) protocol will be explored in this article to avoid data conflict as well as improve bandwidth utilization.

As another method for handling the limitation of communication bandwidth, ETMs will actively reduce the volume of data sent to the network by designing suitable event-triggering conditions. Following ETMs, only the signals with the fluctuations that exceed the preset thresholds will be delivered to the network, and thus, the communication constraints can be effectively alleviated [17]. Compared to the traditional static ETMs (SETMs) with fixed thresholds, dynamic ETMs (DETMs), where the thresholds will be adaptively regulated based on real-time system states, have gained increasing attention [18]. In the existing studies, some research endeavors have been invested in DETM-based control issue of fuzzy SPSs [19], [20]. It is also worth noting that the investigation on integrating the communication protocol with ETM has been conducted to address bandwidth limitation more efficiently [21], [22]. Motivated by this, a novel DETM will be presented and then combined with the MWTOD protocol to assist the studied SMC approach in responding to the communication constraints in this article.

Besides the communication constraints, the security issue incurred by stochastic cyberattacks also profoundly affects the study of the SMC approach. In practice, there are various types of attacks posing threats to the security of NCSs, and the typical among them include deception attacks, denial-of-service (DoS) attacks, and false data injection (FDI) attacks. By injecting falsified data into systems, FDI attacks can deceive the control decisions and then disrupt the normal operation of the systems [23]. Given the unique challenge presented by FDI attacks, the corresponding secure SMC methods have been proposed in the literature. For example, Li and Chen [24] solved the interregional oscillation problem via constructing a robust sliding mode controller for wide-area power systems with FDI attacks; in [25], a terminal integral adaptive SMC method was offered to tackle the tracking control problem of NCSs subject to FDI attacks. Although these valuable results have been presented, but to the best of authors' knowledge, the observer-based SMC problem for fuzzy SPSs with FDI attacks has not been considered, which is another motivation of this work.

Last but not least, another important aspect that needs to be considered in studying SMC is to optimize the parameters of SMC methods to achieve the best control performance. Toward this end, some intelligent optimization algorithms have been successfully applied [26], [27]. In particular, the adaptive particle swarm optimization (APSO) algorithm is widely recognized given its ease of implementation, adaptability, and efficiency [28]. It is further found that by incorporating dynamic learning methods, such as adaptive parameter tuning law and dynamic search strategy, into the APSO algorithm, the reduced parameter dependence and improved convergence speed can be obtained in optimizing SMC [29], [30]. Thus, this article will construct a proper sliding surface and then optimize the sliding domain based on a dynamic learning-based APSO algorithm. Meanwhile, given that the SPP is a critical factor that influences the effectiveness of the SMC strategy [31], the envisioned optimization process also takes the SPP into consideration, which is untouched in the existing works.

Summing up the above discussions, we will dedicate to study dynamic learning-based SMC problem over observer-assisted fuzzy SPSs subject to FDI attacks and limited communication bandwidth in this article. The major contributions of this work can be listed as follows.

1) To comprehensively mitigate the communication constraints, a novel DETM is proposed to actively reduce the transmission of redundant data; furthermore, an MWTOD protocol is presented to achieve collision-free scheduling of the event-triggered signals under a multichannel communication environment.
2) By further considering the influence of the SPP and stochastic FDI attacks, an observer-based sliding surface is constructed, which is followed by the design of a fuzzy SMC strategy.
3) The ε-independent sufficient conditions of achieving the asymptotic stability with guaranteed H_∞ performance and reachability of the sliding surface for the considered fuzzy SPS are analyzed; accordingly, a method for deriving the gains of the established observer and controller is then presented.
4) A dynamic learning-based APSO algorithm is devised to search appropriate values of the SPP and sliding parameters for obtaining optimal control efficiency.

The rest of this article is organized as follows. In Section II, the system model is first introduced, which is followed by the formulation of the studied SMC problem. In Section III, the secure observer-based SMC strategy is presented with the stability and reachability analysis. The proposed dynamic learning-based APSO algorithm that aims to minimize the sliding domain is introduced in Section IV. The simulation

results are demonstrated in Section V. The conclusion of this article and some future works are given in Section VI.

II. System Description and Problem Formulation

In this section, we first introduce the T–S fuzzy model for a nonlinear SPS. Then, the DETM and MWTOD used for easing the communication constraints are described successively. Finally, the considered SMC problem is formulated based on constructing an observer-assisted SMC principle.

A. T–S Fuzzy SPS Model

We consider a nonlinear SPS described by a T–S fuzzy model with r rules, and the ith ($i = 1, 2, \ldots, r$) rule is depicted as follows.

Plant Rule i: IF $h_1(k)$ is $\mathcal{K}_{i1}$ and $h_2(k)$ is $\mathcal{K}_{i2}\cdots$ and $h_q(k)$ is $\mathcal{K}_{iq}$, THEN

$$\begin{aligned} x(k+1) &= A_i E_\varepsilon x(k) + B_i u(k) + D_i w(k) \\ y(k) &= C_i E_\varepsilon x(k) + F_i w(k) \\ z(k) &= H_i E_\varepsilon x(k) \end{aligned} \tag{1}$$

where $h_d(k)(d = 1, 2, \ldots, q)$ are the premise variable vectors and $\mathcal{K}_{id}$ denote the fuzzy sets; $x(k) \triangleq \left[x_s^{\mathrm{T}}(k)\ x_f^{\mathrm{T}}(k)\right]^{\mathrm{T}} \in \mathbb{R}^{n_x}$ is the system state vector; $x_s(k) \in \mathbb{R}^{n_s}$ and $x_f(k) \in \mathbb{R}^{n_f}(n_s + n_f = n_x)$ are the system slow and fast state vectors, respectively; $u(k) \in \mathbb{R}^{n_u}$ is the control input; $y(k) \in \mathbb{R}^{n_y}$ is the measured output; $z(k) \in \mathbb{R}^{n_z}$ represents the controlled output; $\omega(k) \in \mathbb{R}^{n_\omega}$ indicates the disturbance input that belongs to $\mathbb{L}_2[0, \infty)$; $E_\varepsilon \triangleq \mathrm{diag}\{I_{n_s}, \varepsilon I_{n_f}\}$ with $\varepsilon \in (0, \bar{\varepsilon}]$, and $\bar{\varepsilon}$ is the upper-bound of the SPP; and A_i, B_i, C_i, D_i, F_i, and H_i are the constant matrices with appropriate dimensions.

Denoting $h(k) = [h_1(k), h_2(k), \ldots, h_q(k)]^{\mathrm{T}}$ and applying the weighted defuzzification process, the overall fuzzy SPS is then presented as

$$\begin{aligned} x(k+1) &= \sum_{i=1}^{r} \nabla_i(h(k)) \left[A_i E_\varepsilon x(k) + B_i u(k) + D_i w(k)\right] \\ y(k) &= \sum_{i=1}^{r} \nabla_i(h(k)) [C_i E_\varepsilon x(k) + F_i w(k)] \\ z(k) &= \sum_{i=1}^{r} \nabla_i(h(k)) H_i E_\varepsilon x(k) \end{aligned} \tag{2}$$

where $\nabla_i(h(k))$ refers to the standard membership function given by

$$\nabla_i(h(k)) = \frac{\prod_{d=1}^{q} \mathcal{W}_{id}(h_d(k))}{\sum_{i=1}^{r} \prod_{d=1}^{q} \mathcal{W}_{id}(h_d(k))}$$

with $\mathcal{W}_{id}(h_d(k))$ that denotes the grade of membership of $h_d(k)$ in $\mathcal{K}_{id}$. For all k, there exist $\nabla_i(h(k)) \geq 0$, and it is clear that $\sum_{i=1}^{r} \nabla_i(h(k)) = 1$.

B. Demonstration of the DETM and MWTOD Protocol

As shown in Fig. 1, the measured output $y(k)$, which is supposed to be sensed by n_y sensors, i.e., $y(k) = [y_1(k), y_2(k), \ldots, y_{n_y}(k)]^{\mathrm{T}}$ and $y_l(k)$ represents the lth dimension of $y(k)(l = 1, 2, \ldots, n_y)$, is transmitted through the multichannel-enabled communication network with limited bandwidth. Hence, an event detector with the designed DETM is employed to reduce the transmission of redundant data so as to save the communication bandwidth. According to the DETM, only the measurement signals satisfying the following condition can be released:

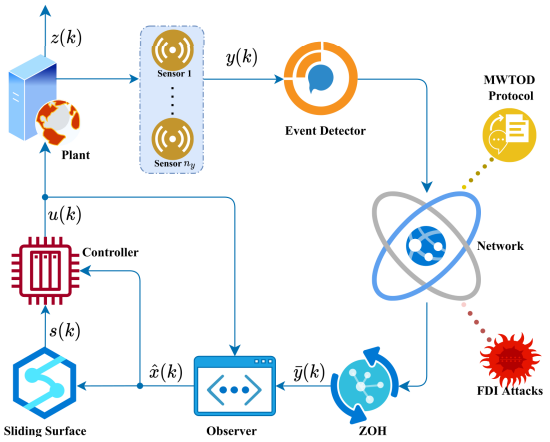

Fig. 1. Envisioned SMC framework.

$$q^{\mathrm{T}}(k)q(k) - \psi(k)y^{\mathrm{T}}(k)y(k) > 0 \tag{3}$$

where $q(k) = y(k) - y(t_m)$ represents the gap between the current measured signal $y(k)$ and the latest triggered signal $y(t_m)$, and $\psi(k)$ is defined as

$$\psi(k) = \psi_1 + \psi_2 e^{-\rho\|y(k) - y(t_m)\|} \tag{4}$$

in which ψ_1, ψ_2, and ρ are the given positive parameters. Obviously, $\psi_1 \leq \psi(k) \leq \psi_1 + \psi_2 \triangleq \psi_3$. If the event-triggering sequence is represented as $0 = t_0 < t_1 < t_2 < \cdots < t_m < \cdots$ and t_m indicates the latest event-triggering instant, then the next event-triggering instant t_{m+1} can be expressed as

$$t_{m+1} = \min_{k \in \mathbb{N}^+} \{k | k > t_m \ \&\& \ (3) \text{ is satisfied at time instant } k\}. \tag{5}$$

Remark 1: If the event-triggering condition (3) is met during data transmission, the current measurable signal $y(k)$ will be released; otherwise, the signal will be regarded as redundant data and discarded promptly. Furthermore, the larger the gap between $y(k)$ and $y(t_m)$, the smaller the value of $\psi(k)$, which indicates that $y(k)$ is more likely to be delivered with the satisfaction of the condition (3).

At each event-triggering instant t_m ($m = 1, 2, \ldots,$), however, not every dimension of $y(t_m)$ can be successfully transmitted over the multichannel-enabled bandwidth-limited communication network. Supposing that there are n ($n < n_y$) available channels, the signals generated by n_y sensors should be seriously scheduled to avoid data collision. In view of this, the MWTOD protocol is proposed to appropriately arrange the data transmission at each t_m. Let $J(t_m) = \{\kappa_1(t_m), \kappa_2(t_m), \ldots, \kappa_n(t_m)\}$ be the set of indexes of the sensors, which are allowed to transmit the generated signals at t_m; each of the authorized sensor will be assigned a dedicated channel

for data transmission, and then, the scheduling rule of the MWTOD protocol is formulated as follows:

$$\kappa_w(t_m) = \arg\max_{h\in\Omega_w} \left(y_h(t_m) - y_h^*(t_m)\right)^{\mathrm{T}} W \times \left(y_h(t_m) - y_h^*(t_m)\right) \tag{6}$$

where $y_h^*(t_m)$ indicates the latest transmitted signal from sensor h before event-triggered instant t_m; $w = 1, 2, \ldots, n$; W is a given positive weight matrix; and $\Omega_1 = \{1, 2, \ldots, n_y\}$ and $\Omega_w = \Omega_{w-1} \setminus \{\kappa_{w-1}(t_m)\}$ for $w > 1$. It is obvious that there are U possible scenarios for $J(t_m)$, i.e., $J(t_m) \in J = \{J^1, J^2, \ldots, J^U\}$, where $U = C(n_y, n)$ denotes the combination of n_y choose n, and each J^t $(t = 1, 2, \ldots, U)$ is a set of sensor indexes with $|J^t| = n$.

Based on the MWTOD protocol and employing a zero-order-holder (ZOH) as shown in Fig. 1, $y_l(t_m)$ $(l = 1, 2, \ldots, n_y)$ can be renewed as

$$\bar{y}_l(t_m) = \begin{cases} y_l(t_m), & \text{if } l \in J(t_m) \\ \bar{y}_l(t_{m-1}), & \text{otherwise.} \end{cases} \tag{7}$$

Here, we assume that $\bar{y}_l(t_0) = y_l(t_0)$ for easy derivation.

Remark 2: In this study, the DETM is first implemented to reduce the redundant transmission of the measurement signal based on the condition (3), and then, the MWTOD protocol presented by (6) is applied to enable that each available channel is exactly matched with one sensor to avoid data collision at event-triggering instants. The combined use of the two strategies refines the original measurement signal, which, in turn, informs the design of the subsequent SMC method, so the effective SMC performance under the limited communication bandwidth can be expected.

C. Formal Description of the FDI Attacks

For the sensors that are scheduled to transfer measurement information, it is considered that the data transmission of them is compromised by FDI attacks. Given the stochastic feature of the attacks, a Bernoulli variable $\alpha(k)$ with the following probability distribution:

$$\mathrm{Prob}\{\alpha(k) = 1\} = \bar{\alpha}, \quad \mathrm{Prob}\{\alpha(k) = 0\} = 1 - \bar{\alpha} \tag{8}$$

is used to depict the occurrence of the FDI attacks, where $\bar{\alpha} \in [0, 1]$. To be specific, $\alpha(k) = 1$ indicates the successful injection of the false data at time instant k, and vice versa. Furthermore, an energy-bounded function $\mathcal{I}(k) = \left[\mathcal{I}_1(k), \mathcal{I}_2(k), \ldots, \mathcal{I}_{n_y}(k)\right]^{\mathrm{T}}$, which fulfills the following condition:

$$\|\mathcal{I}(k)\| \le \|My(k)\| \tag{9}$$

is adopted to characterize the attack signals. Under the effect of the formulated attacks, $\bar{y}_l(t_m)$ given in (7) is updated as

$$\bar{y}_l(t_m) = \begin{cases} y_l(t_m) + \alpha(t_m)\mathcal{I}_l(t_m), & \text{if } \quad l \in J(t_m) \\ \bar{y}_l(t_{m-1}), & \text{otherwise.} \end{cases} \tag{10}$$

To achieve an augmented formulation, the following matrix is defined first:

$$\Phi_{\varphi(t_m)} = \sum_{w=1}^{n} \chi_{\kappa_w(t_m)} \tag{11}$$

where $\chi_{\kappa_w(t_m)} = \mathrm{diag}\{\delta(\kappa_w(t_m) - 1), \ldots, \delta(\kappa_w(t_m) - n_y)\}$, $\delta(\cdot) \in \{0, 1\}$ is a Kronecker delta function, and $\varphi(t_m) = t$ if $J(t_m) = J^t$ $(t = 1, 2, \ldots, U)$. Then, the measured output received by the observer can be formulated as

$$\bar{y}(t_m) = \Phi_{\varphi(t_m)} y(t_m) + \alpha(t_m)\Phi_{\varphi(t_m)}\mathcal{I}(t_m) + \bar{\Phi}_{\varphi(t_m)}\bar{y}(t_{m-1}) \tag{12}$$

where $\bar{\Phi}_{\varphi(t_m)} = I - \Phi_{\varphi(t_m)}$.

D. Design of the Observer-Based Sliding Surface

Given the application of ZOH strategy, for $k \in [t_m, t_{m+1})$ $(m = 0, 1, 2, \ldots)$, it can be found that $\bar{y}(k) = \bar{y}(t_m)$. Thus, without loss of generality, the following derivation and analysis will concentrate on the interval $[t_m, t_{m+1})$. For the envisioned T–S fuzzy SPS, the observer with r rules is constructed as follows.

Observer Rule i: IF $h_1(k)$ is $\mathcal{K}_{i1}$ and $h_2(k)$ is $\mathcal{K}_{i2} \cdots$ and $h_q(k)$ is $\mathcal{K}_{iq}$, THEN

$$\begin{aligned} \hat{x}(k+1) &= A_i E_\varepsilon \hat{x}(k) + B_i u(k) + B_i \sum_{j=1}^{r} \nabla_j(h(k)) \\ &\quad \times L_{j,\varphi(k)}(\bar{y}(k) - \hat{y}(k)) \\ \hat{y}(k) &= C_i E_\varepsilon \hat{x}(k) \end{aligned} \tag{13}$$

where $i = 1, 2, \ldots, r$; $\hat{x}(k) \triangleq \left[\hat{x}_s^{\mathrm{T}}(k) \;\; \hat{x}_f^{\mathrm{T}}(k)\right]^{\mathrm{T}} \in \mathbb{R}^{n_s+n_f}$ and $\hat{y}(k) \in \mathbb{R}^{n_y}$, respectively, represent the observations of $x(k)$ and $y(k)$; $\varphi(k) = \varphi(t_m)$; and $L_{j,\varphi(k)}$ are the observer gains, which will be designed shortly. By introducing the standard membership function, the fuzzy observer can be given as

$$\begin{aligned} \hat{x}(k+1) &= \sum_{i=1}^{r} \nabla_i(h(k)) \Big[A_i E_\varepsilon \hat{x}(k) + B_i u(k) \\ &\quad + B_i \sum_{j=1}^{r} \nabla_j(h(k)) L_{j,\varphi(k)}(\bar{y}(k) - \hat{y}(k))\Big] \\ \hat{y}(k) &= \sum_{i=1}^{r} \nabla_i(h(k)) C_i E_\varepsilon \hat{x}(k). \end{aligned} \tag{14}$$

Based on (14), the fuzzy sliding surface function is then designed as follows:

$$\begin{aligned} s(k+1) &= \sum_{i=1}^{r}\sum_{j=1}^{r} \nabla_i(h(k))\nabla_j(h(k)) \\ &\quad \times \Big[G\hat{x}(k+1) - G\left(A_i + B_i K_{j,\varphi(k)} \right. \\ &\quad \left. - B_i L_{j,\varphi(k)} C_i\right) E_\varepsilon \hat{x}(k)\Big] \end{aligned} \tag{15}$$

where G is a real matrix which will be chosen to guarantee that GB_i is nonsingular and $K_{j,\varphi(k)}$ are the controller gains, which need to be determined.

E. Problem Formulation

To achieve a simpler and more practical form of control, the following fuzzy equivalent SMC law is devised by taking the ideal sliding motion premise, where $s(k+1) = s(k) = 0$ into consideration [13], [32]:

$$u_{eq}(k) = \sum_{j=1}^{r} \nabla_j(h(k)) \left[K_{j,\varphi(k)} E_\varepsilon \hat{x}(k) - L_{j,\varphi(k)} \bar{y}(k)\right]. \tag{16}$$

Then, by replacing $u(k)$ in both (2) and (14) with $u_{eq}(k)$, it can be gotten that

$$x(k+1) = \sum_{i=1}^{r}\sum_{j=1}^{r} \nabla_i(h(k))\nabla_j(h(k)) \left[A_i E_\varepsilon x(k) + B_i \times K_{j,\varphi(k)} E_\varepsilon \hat{x}(k) - B_i L_{j,\varphi(k)} \bar{y}(k) + D_i w(k)\right] \tag{17}$$

$$\hat{x}(k+1) = \sum_{i=1}^{r}\sum_{j=1}^{r} \nabla_i(h(k))\nabla_j(h(k)) \left[A_i + B_i K_{j,\varphi(k)} - B_i L_{j,\varphi(k)} C_i\right] E_\varepsilon \hat{x}(k). \tag{18}$$

Letting $e(k) \triangleq x(k) - \hat{x}(k)$ be the observer error, and recurring to (2), (12), (17), and (18), and then, it has

$$\begin{aligned} e(k+1) &= x(k+1) - \hat{x}(k+1) \\ &= \sum_{i=1}^{r}\sum_{j=1}^{r} \nabla_i(h(k))\nabla_j(h(k)) \\ &\quad \times \left[A_i E_\varepsilon e(k) + D_i w(k) + B_i L_{j,\varphi(k)} C_i E_\varepsilon \hat{x}(k) - B_i L_{j,\varphi(k)} \bar{y}(k)\right] \\ &= \sum_{i=1}^{r}\sum_{j=1}^{r} \nabla_i(h(k))\nabla_j(h(k)) \\ &\quad \times \Big[\left(A_i - B_i L_{j,\varphi(k)} \Phi_{\varphi(k)} \times C_i\right) E_\varepsilon e(k) \\ &\quad + B_i L_{j,\varphi(k)} \bar{\Phi}_{\varphi(k)} C_i E_\varepsilon \hat{x}(k) \\ &\quad + (D_i - B_i L_{j,\varphi(k)} \Phi_{\varphi(k)} F_i) w(k) - B_i L_{j,\varphi(k)} \\ &\quad \left(\bar{\Phi}_{\varphi(k)} \times \bar{y}(t_{m-1}) + \alpha(t_m) \Phi_{\varphi(k)} \mathcal{I}(t_m) - \Phi_{\varphi(k)} q(k)\right)\Big]. \end{aligned} \tag{19}$$

Defining $\xi(k) = \left[\hat{x}^{\mathrm{T}}(k) \;\; e^{\mathrm{T}}(k) \;\; \bar{y}^{\mathrm{T}}(t_{m-1})\right]^{\mathrm{T}}$, then an augmented T–S fuzzy SPS can be inferred as follows:

$$\begin{aligned} \xi(k+1) &= \sum_{i=1}^{r}\sum_{j=1}^{r} \nabla_i(h(k))\nabla_j(h(k)) \\ &\quad \times \left[\mathcal{F}_{ijt\varepsilon}\xi(k) + \left(\mathcal{E}_{1ijt} + \mathcal{E}_{2ijt\varepsilon}\right)\mathcal{U}(k)\right] \\ z(k) &= \sum_{i=1}^{r} \nabla_i(h(k)) \mathcal{H}_{i\varepsilon}\xi(k) \end{aligned} \tag{20}$$

where

$$\begin{aligned} \mathcal{U}(k) &= \left[w^{\mathrm{T}}(k) \quad q^{\mathrm{T}}(k) \quad \mathcal{I}^{\mathrm{T}}(t_m)\right]^{\mathrm{T}} \\ \mathcal{H}_{i\varepsilon} &= \left[H_i E_\varepsilon \quad H_i E_\varepsilon \quad 0\right] \\ \mathcal{F}_{ijt\varepsilon} &= \begin{bmatrix} \mathcal{T}_{1ijt} E_\varepsilon & 0 & 0 \\ \mathcal{T}_{2ijt} C_i E_\varepsilon & \mathcal{T}_{3ijt} E_\varepsilon & \mathcal{T}_{4ijt} \\ \Phi_{\varphi(k)} C_i E_\varepsilon & \Phi_{\varphi(k)} C_i E_\varepsilon & \bar{\Phi}_{\varphi(k)} \end{bmatrix} \\ \mathcal{E}_{1ijt} &= \begin{bmatrix} 0 & 0 & 0 \\ D_i - \mathcal{T}_{5ijt} F_i & \mathcal{T}_{5ijt} & -\bar{\alpha}\mathcal{T}_{5ijt} \\ \Phi_{\varphi(k)} F_i & -\Phi_{\varphi(k)} & \bar{\alpha}\Phi_{\varphi(k)} \end{bmatrix} \\ \mathcal{E}_{2ijt} &= \left[0 \quad 0 \quad \mathcal{D}_{ijt}\right] \\ \mathcal{T}_{1ijt} &= A_i + B_i K_{j,\varphi(k)} - B_i L_{j,\varphi(k)} C_i \\ \mathcal{T}_{2ijt} &= B_i L_{j,\varphi(k)} \bar{\Phi}_{\varphi(k)}, \quad \mathcal{T}_{3ijt} = A_i - B_i L_{j,\varphi(k)} \Phi_{\varphi(k)} C_i \\ \mathcal{T}_{4ijt} &= -B_i L_{j,\varphi(k)} \bar{\Phi}_{\varphi(k)}, \quad \mathcal{T}_{5ijt} = B_i L_{j,\varphi(k)} \Phi_{\varphi(k)} \\ \mathcal{D}_{ijt} &= \left[0 \quad -\tilde{\alpha}(t_m)\mathcal{T}_{5ijt}^{\mathrm{T}} \quad \tilde{\alpha}(t_m)\Phi_{\varphi(k)}^{\mathrm{T}}\right]^{\mathrm{T}} \\ \tilde{\alpha}(t_m) &= \alpha(t_m) - \bar{\alpha}, \quad t = 1, 2, \ldots, U. \end{aligned}$$

Based on the system (20), this article then devotes to design appropriate observer and controller gains to ensure that the system is asymptotically stable with guaranteed H_∞ performance and achieves the reachability of the sliding surface in accordance with the designed sliding surface function (15). At the end of this section, the following lemmas are presented to assist the subsequent analysis.

Lemma 1 [33]: Given a full rank matrix $\mathbb{B} \in \mathbb{R}^{n_x \times n_u}$, the singular value decomposition (SVD) for which can be expressed as

$$\mathbb{B} = \mathbb{O}\begin{bmatrix}\mathbb{S} \\ 0\end{bmatrix}\mathbb{V}^{\mathrm{T}}$$

where $\mathbb{O}^{\mathrm{T}}\mathbb{O} = I$ and $\mathbb{V}^{\mathrm{T}}\mathbb{V} = I$, for matrices $\mathbb{H} > 0$, $\mathbb{D} \in \mathbb{R}^{n_x \times n_x}$, and $\mathbb{E} \in \mathbb{R}^{n_u \times n_x}$, there has a matrix $\bar{\mathbb{H}}$ such that $\mathbb{H}\mathbb{B} = \mathbb{B}\bar{\mathbb{H}}$ holds if and only if

$$\mathbb{H} = \mathbb{O}\begin{bmatrix}\mathbb{D} & 0 \\ 0 & \mathbb{E}\end{bmatrix}\mathbb{O}^{\mathrm{T}}.$$

Lemma 2 [34]: Given a positive scalar ε and symmetric matrices Z_1 and Z_2, if $Z_1 \le 0$ and $Z_1 + \bar{\varepsilon} Z_2 < 0$, then it has

$$Z_1 + \varepsilon Z_2 < 0 \text{ for } \quad \forall \varepsilon \in (0, \bar{\varepsilon}].$$

III. Proposed SMC Method

In this section, the sufficient conditions for stabilizing the SPS (20) are derived in Theorem 1 first. Then, the analysis of the reachability of the sliding surface is presented by Theorem 2. An observer-based T–S fuzzy SMC method is finally given by calculating the observer and controller gains in Theorem 3. The derivation also focuses on the interval $[t_m, t_{m+1})$.

Theorem 1: Given scalars $\psi_1 > 0$, $\psi_2 > 0$, $\varepsilon > 0$, $\gamma > 0$, $\bar{\alpha} \in [0, 1]$, observer, and controller gains $L_{j,t}$ and $K_{j,t}(j = 1, 2, \ldots, r; t = 1, 2, \ldots, U)$, the asymptotically stability with guaranteed H_∞ performance of the augmented T–S fuzzy SPS (20) can be achieved if there exist positive-define matrices Ψ_t with compatible dimensions so that the following matrix inequalities hold:

$$\mathbb{X}_{ijt\varepsilon} = \begin{bmatrix} \Gamma_{1ijt\varepsilon} - \Psi_t + \mathcal{A}_1 + \mathcal{B} & * \\ \Gamma_{2ijt\varepsilon} + \mathcal{A}_2 & \Gamma_{3ijt} + \mathcal{A}_3 + \mathcal{F} \end{bmatrix} < 0 \tag{21}$$

where

$$\begin{aligned} \Gamma_{1ijt\varepsilon} &= \mathcal{F}_{ijt\varepsilon}^{\mathrm{T}} \Psi_h \mathcal{F}_{ijt\varepsilon}, \quad \Gamma_{2ijt\varepsilon} = \mathcal{E}_{1ijt}^{\mathrm{T}} \Psi_h \mathcal{F}_{ijt\varepsilon} \\ \Gamma_{3ijt} &= \mathcal{E}_{1ijt}^{\mathrm{T}} \Psi_h \mathcal{E}_{1ijt} + \bar{\mathcal{E}}_{2ijt}^{\mathrm{T}} \Psi_h \bar{\mathcal{E}}_{2ijt} \\ \bar{\mathcal{E}}_{2ijt} &= \left[0 \quad 0 \quad \bar{\mathcal{D}}_{ijt}\right] \\ h &= \begin{cases} t = \varphi(t_m), & \text{if } k \in [t_m, t_{m+1} - 1) \\ \varphi(t_{m+1}), & \text{if } k = t_{m+1} - 1 \end{cases} \\ \mathcal{A}_1 &= \begin{bmatrix} E_\varepsilon^{\mathrm{T}} C_i^{\mathrm{T}} \Theta_1 C_i E_\varepsilon & * & * \\ E_\varepsilon^{\mathrm{T}} C_i^{\mathrm{T}} \Theta_1 C_i E_\varepsilon & E_\varepsilon^{\mathrm{T}} C_i^{\mathrm{T}} \Theta_1 C_i E_\varepsilon & * \\ 0 & 0 & 0 \end{bmatrix} \\ \mathcal{A}_2 &= \begin{bmatrix} F_i^{\mathrm{T}} \Theta_1 C_i E_\varepsilon & F_i^{\mathrm{T}} \Theta_1 C_i E_\varepsilon & 0 \\ -M^{\mathrm{T}} M C_i E_\varepsilon & -M^{\mathrm{T}} M C_i E_\varepsilon & 0 \\ 0 & 0 & 0 \end{bmatrix} \\ \mathcal{A}_3 &= \begin{bmatrix} F_i^{\mathrm{T}} \Theta_1 F_i & * & * \\ -M^{\mathrm{T}} M F_i & M^{\mathrm{T}} M - I & * \\ 0 & 0 & -I \end{bmatrix} \end{aligned}$$

$$\mathcal{B} = \begin{bmatrix} E_\varepsilon^{\mathrm{T}} H_i^{\mathrm{T}} H_i E_\varepsilon & * & * \\ E_\varepsilon^{\mathrm{T}} H_i^{\mathrm{T}} H_i E_\varepsilon & E_\varepsilon^{\mathrm{T}} H_i^{\mathrm{T}} H_i E_\varepsilon & * \\ 0 & 0 & 0 \end{bmatrix}$$
$$\bar{\mathcal{D}}_{ijt} = \begin{bmatrix} 0 & -\sqrt{\bar{\alpha}\vec{\alpha}}(B_i L_{j,t}\Phi_t)^{\mathrm{T}} & \sqrt{\bar{\alpha}\vec{\alpha}}\Phi_t^{\mathrm{T}} \end{bmatrix}^{\mathrm{T}}$$
$$\mathcal{F} = \mathrm{diag}\{-\gamma^2 I, 0, 0\}$$
$$\Theta_1 = M^{\mathrm{T}}M + \psi_3 I, \quad \vec{\alpha} = 1 - \bar{\alpha}, \quad i = 1, 2, \ldots, r.$$

Proof: We construct the following Lyapunov function:

$$V_1(k) = \boldsymbol{\xi}^{\mathrm{T}}(k)\Psi_t \boldsymbol{\xi}(k) \tag{22}$$

and then, define the forward difference of $V_1(k)$ as $\Delta V_1(k) \triangleq V_1(k+1) - V_1(k)$.

According to (8), and further considering the event-triggering condition (3) and the upper bound of the FDI attack signals (9), it can be derived that

$$\begin{aligned}
&E\{\Delta V_1(k)\} \\
&= E\left\{\xi^{\mathrm{T}}(k+1)\Psi_h \xi(k+1) - \xi^{\mathrm{T}}(k)\Psi_t \xi(k)\right\} \\
&\le E\left\{\xi^{\mathrm{T}}(k+1)\Psi_h \xi(k+1) - \xi^{\mathrm{T}}(k)\Psi_t \xi(k) + (y(k) \right. \\
&\qquad - q(k))^{\mathrm{T}} M^{\mathrm{T}} M (y(k) - q(k)) - \mathcal{I}^{\mathrm{T}}(t_m)\mathcal{I}(t_m) \\
&\qquad \left. + \psi_3 y^{\mathrm{T}}(k) \times y(k) - q^{\mathrm{T}}(k) q(k)\right\} \\
&= E\left\{\sum_{i=1}^{r}\sum_{j=1}^{r} \nabla_i(h(k))\nabla_j(h(k)) \right. \\
&\qquad \times \left[\mathcal{F}_{ijt\varepsilon}\xi(k) + (\mathcal{E}_{1ijt} + \mathcal{E}_{2ijt}) \times \mathcal{U}(k)\right]^{\mathrm{T}} \\
&\qquad \times \Psi_h \left[\mathcal{F}_{ijt\varepsilon}\xi(k) + (\mathcal{E}_{1ijt} + \mathcal{E}_{2ijt})\mathcal{U}(k)\right] - \xi^{\mathrm{T}}(k)\Psi_t \\
&\qquad \times \xi^{\mathrm{T}}(k) + y^{\mathrm{T}}(k)(M^{\mathrm{T}}M + \psi_3 I) y(k) \\
&\qquad + q^{\mathrm{T}}(k)(M^{\mathrm{T}}M - I) q(k) - y^{\mathrm{T}}(k) M^{\mathrm{T}} M q(k) \\
&\qquad \left. - q^{\mathrm{T}}(k) M^{\mathrm{T}} M y(k) - \mathcal{I}^{\mathrm{T}}(t_m)\mathcal{I}(t_m)\right\} \\
&= \sum_{i=1}^{r}\sum_{j=1}^{r} \nabla_i(h(k))\nabla_j(h(k)) \left[\zeta^{\mathrm{T}}(k)\mathcal{M}_{ijt\varepsilon}\zeta(k)\right]
\end{aligned} \tag{23}$$

where

$$\zeta(k) = \begin{bmatrix} \xi^{\mathrm{T}}(k) & \mathcal{U}^{\mathrm{T}}(k) \end{bmatrix}^{\mathrm{T}}$$
$$\mathcal{M}_{ijt\varepsilon} = \begin{bmatrix} \Gamma_{1ijt\varepsilon} + \mathcal{A}_1 & * \\ \Gamma_{2ijt\varepsilon} + \mathcal{A}_2 & \Gamma_{3ijt} + \mathcal{A}_3 \end{bmatrix}.$$

Based on the control output given in (20), we then can readily get

$$\begin{aligned}
&E\{\Delta V_1(k)\} + z^{\mathrm{T}}(k)z(k) - \gamma^2 w^{\mathrm{T}}(k)w(k) \\
&\le \sum_{i=1}^{r}\sum_{j=1}^{r} \nabla_i(h(k))\nabla_j(h(k)) \left[\zeta^{\mathrm{T}}(k)\mathbb{X}_{ijt\varepsilon}\zeta(k)\right].
\end{aligned} \tag{24}$$

Thus, if the condition (21) is satisfied, it is clear that

$$E\{\Delta V_1(k)\} + z^{\mathrm{T}}(k)z(k) - \gamma^2 w^{\mathrm{T}}(k)w(k) \le 0. \tag{25}$$

Then, while the external disturbance $w(k) = 0$, it can be easily observed that $E\{\Delta V_1(k)\} \le 0$ by using the Schur complement method, which indicates that the system (20) is asymptotically stable. Moreover, by summarizing both sides of (25) for time instant k from 0 to ∞ with the zero initial condition, it can be gotten that

$$\sum_{k=0}^{\infty} \|z(k)\|^2 \le \gamma^2 \sum_{k=0}^{\infty} \|w(k)\|^2 \tag{26}$$

which means that the H_∞ performance with the given disturbance attenuation level γ of the system (20) is assured. So far, the proof of Theorem 1 is completed. ■

Theorem 2: Given scalars $\psi_1 > 0$, $\psi_2 > 0$, $\varepsilon > 0$, $\gamma > 0$, $\mathbf{d} > 0$, $\bar{\alpha} \in [0, 1]$, observer, and controller gains $L_{j,t}$ and $K_{j,t}(j = 1, 2, \ldots, r; t = 1, 2, \ldots, U)$, if there exist positive-define matrices Ψ_t and Q with suitable dimensions, scalars $\nu_1 > 0$ and $\nu_2 > 0$, which can ensure

$$G^{\mathrm{T}} Q G \le \nu_1 I \tag{27}$$
$$B_i^{\mathrm{T}} G^{\mathrm{T}} Q G B_i \le \nu_2 I \tag{28}$$
$$\mathbb{X}_{ijt\varepsilon} + 2\nu_1 \left(\mathcal{N}_{1ijt\varepsilon}^{\mathrm{T}} \mathcal{N}_{1ijt\varepsilon} + \bar{\mathcal{N}}_{2ijt}^{\mathrm{T}} \bar{\mathcal{N}}_{2ijt}\right) < 0. \tag{29}$$

Then, the state trajectories will be directed into the following sliding domain:

$$\mathfrak{C} = \left\{ s(k) \mid \|s(k)\| \le \mathcal{O}(k) \triangleq \sqrt{\frac{2\mathbf{d}^2\nu_2}{\lambda_{\min}(Q)}} \|\bar{y}(k)\| \right\} \tag{30}$$

by constructing the subsequent control law

$$u(k) = \sum_{j=1}^{r} \nabla_j(h(k))[K_{j,t} E_\varepsilon \hat{x}(k) - \mathbf{d}\,\|\bar{y}(k)\|\,\mathrm{sgn}(s(k))] \tag{31}$$

where

$$\mathcal{N}_{1ijt\varepsilon} = \begin{bmatrix} \Upsilon_1\Upsilon_2 & \Upsilon_1\Upsilon_2 & B_i L_{j,t}\bar{\Phi}_t & \Upsilon_1 F_i & -\Upsilon_1 & \bar{\alpha}\Upsilon_1 \end{bmatrix}$$
$$\bar{\mathcal{N}}_{2ijt} = \begin{bmatrix} 0 & 0 & 0 & 0 & 0 & \sqrt{\bar{\alpha}\vec{\alpha}}\Upsilon_1 \end{bmatrix}$$
$$\Upsilon_1 = B_i L_{j,t}\Phi_t, \quad \Upsilon_2 = C_i E_\varepsilon, \quad i = 1, 2, \ldots, r.$$

Proof: We define the Lyapunov function as

$$V(k) = V_1(k) + V_2(k)$$

where $V_2(k) = s^{\mathrm{T}}(k) Q s(k)$. Based on (31), it has

$$\begin{aligned}
&s(k+1) \\
&= \sum_{i=1}^{r}\sum_{j=1}^{r} \nabla_i(h(k))\nabla_j(h(k)) \\
&\quad \times [G\hat{x}(k+1) - G(A_i + B_i K_{j,t} - B_i L_{j,t} C_i) E_\varepsilon \hat{x}(k)] \\
&= \sum_{i=1}^{r}\sum_{j=1}^{r} \nabla_i(h(k))\nabla_j(h(k)) \\
&\quad \times \left[G(A_i E_\varepsilon \hat{x}(k) + B_i u(k) + B_i L_{j,t}(\bar{y}(k) - \hat{y}(k))) \right. \\
&\quad \left. - G(A_i + B_i K_{j,t} - B_i L_{j,t} \times C_i) E_\varepsilon \hat{x}(k)\right] \\
&= \sum_{i=1}^{r}\sum_{j=1}^{r} \nabla_i(h(k))\nabla_j(h(k)) \\
&\quad \times \left[G B_i L_{j,t} \left(\Phi_t(C_i E_\varepsilon \hat{x}(k) + C_i E_\varepsilon e(k) + F_i w(k) - q(k)) \right.\right. \\
&\qquad \left.\left. + \alpha(t_m)\Phi_t \mathcal{I}(t_m) + \bar{\Phi}_t \times \bar{y}(t_{m-1})\right) \right. \\
&\quad \left. - \mathbf{d} G B_i \,\|\bar{y}(k)\|\,\mathrm{sgn}(s(k))\right]
\end{aligned}$$

$$= \sum_{i=1}^{r}\sum_{j=1}^{r} \nabla_i(h(k))\nabla_j(h(k)) \times [G(\mathcal{N}_{1ijt\varepsilon} + \mathcal{N}_{2ijt}) \times \zeta(k) - \mathbf{d}GB_i \|\bar{y}(k)\| \operatorname{sgn}(s(k))] \quad (32)$$

where $\mathcal{N}_{2ijt} = \begin{bmatrix} 0 & 0 & 0 & 0 & 0 & \tilde{\alpha}(t_m)\Upsilon_1 \end{bmatrix}$.

Let $\Delta V_2(k) \triangleq V_2(k+1) - V_2(k)$, and according to the conditions (27) and (28), it can be derived that

$$\begin{aligned} E\{\Delta V_2(k)\} &= E\left\{s^{\mathrm{T}}(k+1)Qs(k+1) - s^{\mathrm{T}}(k)Qs(k)\right\} \\ &= E\left\{\sum_{i=1}^{r}\sum_{j=1}^{r} \nabla_i(h(k))\nabla_j(h(k)) \right. \\ &\quad \left\{[G(\mathcal{N}_{1ijt\varepsilon} + \mathcal{N}_{2ijt})\zeta(k) - \mathbf{d}GB_i \|\bar{y}(k)\| \operatorname{sgn}(s(k))]^{\mathrm{T}} \right. \\ &\quad Q[G(\mathcal{N}_{1ijt\varepsilon} + \mathcal{N}_{2ijt})\zeta(k) - \mathbf{d}GB_i \|\bar{y}(k)\| \operatorname{sgn}(s(k))] \\ &\quad \left.\left. - s^{\mathrm{T}}(k)Qs(k)\right\}\right\} \\ &\le E\left\{\sum_{i=1}^{r}\sum_{j=1}^{r} \nabla_i(h(k))\nabla_j(h(k))2\nu_1[(\mathcal{N}_{1ijt\varepsilon} + \mathcal{N}_{2ijt})\zeta(k)]^{\mathrm{T}} \right. \\ &\quad \times [(\mathcal{N}_{1ijt\varepsilon} + \mathcal{N}_{2ijt})\zeta(k)] + 2\mathbf{d}^2\nu_2 \|\bar{y}(k)\|^2 - \lambda_{\min}(Q) \\ &\quad \left.\times \|s(k)\|^2\right\} \\ &= \sum_{i=1}^{r}\sum_{j=1}^{r} \nabla_i(h(k))\nabla_j(h(k))2\nu_1\zeta^{\mathrm{T}}(k) \\ &\quad \times \left(\mathcal{N}_{1ijt\varepsilon}^{\mathrm{T}}\mathcal{N}_{1ijt\varepsilon} + \bar{\mathcal{N}}_{2ijt}^{\mathrm{T}}\bar{\mathcal{N}}_{2ijt}\right)\zeta(k) + 2\mathbf{d}^2\nu_2 \|\bar{y}(k)\|^2 \\ &\quad - \lambda_{\min}(Q)\|s(k)\|^2. \end{aligned} \quad (33)$$

Then, by combining (24) and (33), it can be inferred that

$$\begin{aligned} &E\{\Delta V(k)\} + z^{\mathrm{T}}(k)z(k) - \gamma^2 w^{\mathrm{T}}(k)w(k) \\ &= E\left\{\Delta V_1(k) + z^{\mathrm{T}}(k)z(k) - \gamma^2 w^{\mathrm{T}}(k)w(k) + \Delta V_2(k)\right\} \\ &\le \sum_{i=1}^{r}\sum_{j=1}^{r} \nabla_i(h(k))\nabla_j(h(k)) \\ &\quad \times \left\{\zeta^{\mathrm{T}}(k)\mathbb{X}_{ijt\varepsilon}\zeta(k) + 2\nu_1\zeta^{\mathrm{T}}(k)\right. \\ &\quad \times \left(\mathcal{N}_{1ijt\varepsilon}^{\mathrm{T}}\mathcal{N}_{1ijt\varepsilon} + \bar{\mathcal{N}}_{2ijt}^{\mathrm{T}}\bar{\mathcal{N}}_{2ijt}\right)\zeta(k) + 2\mathbf{d}^2\nu_2\|\bar{y}(k)\|^2 \\ &\quad \left. - \lambda_{\min}(Q)\|s(k)\|^2\right\} \\ &= \sum_{i=1}^{r}\sum_{j=1}^{r} \nabla_i(h(k))\nabla_j(h(k)) \\ &\quad \times \left\{\zeta^{\mathrm{T}}(k)\left[\mathbb{X}_{ijt\varepsilon} + 2\nu_1\left(\mathcal{N}_{1ijt\varepsilon}^{\mathrm{T}} \times \mathcal{N}_{1ijt\varepsilon} + \bar{\mathcal{N}}_{2ijt}^{\mathrm{T}}\bar{\mathcal{N}}_{2ijt}\right)\right]\zeta(k)\right. \\ &\quad \left. - \left[\lambda_{\min}(Q)\|s(k)\|^2 - 2\mathbf{d}^2 \times \nu_2\|\bar{y}(k)\|^2\right]\right\}. \end{aligned} \quad (34)$$

Thus, if $s(k)$ strays from the domain $\mathfrak{C}$, i.e., $\|s(k)\| > \mathcal{O}(k)$, it follows from the condition (29) that:

$$\begin{aligned} &E\{\Delta V(k)\} + z^{\mathrm{T}}(k)z(k) - \gamma^2 w^{\mathrm{T}}(k)w(k) \\ &\le \sum_{i=1}^{r}\sum_{j=1}^{r} \nabla_i(h(k))\nabla_j(h(k))\{\zeta^{\mathrm{T}}(k) \\ &\quad \times \left[\mathbb{X}_{ijt\varepsilon} + 2\nu_1\left(\mathcal{N}_{1ijt\varepsilon}^{\mathrm{T}} \times \mathcal{N}_{1ijt\varepsilon} + \bar{\mathcal{N}}_{2ijt}^{\mathrm{T}}\bar{\mathcal{N}}_{2ijt}\right)\right]\zeta(k) < 0 \end{aligned} \quad (35)$$

which implies that the state trajectories will be driven into the domain $\mathfrak{C}$, and thus, the theorem is validated. ■

It is noteworthy that the main results presented in Theorems 1 and 2 are derived based on the given observer and controller gains, and there are exist nonlinear terms in (29), which makes it difficult to obtain observer-assisted controller parameters via directly solving (29). Moreover, it can be found that (29) is ε-dependent, but the SPP ε is hard to acquire precisely in practice. In view of these, in Theorem 3, the upper bound for the SPP ε, i.e., $\bar{\varepsilon}$, is introduced to get the ε-independent version of (29); meanwhile, the Schur complement method and linear matrix inequality (LMI) technology are adopted to handle the nonlinear terms and then obtain appropriate observer and controller gains.

Theorem 3: Given scalars $\psi_1 > 0$, $\psi_2 > 0$, $\bar{\varepsilon} > 0$, $\gamma > 0\bar{\alpha} \in [0, 1]$, the asymptotically stability with guaranteed H_∞ performance and the reachability of the sliding domain $\mathfrak{C}$ of the augmented T–S fuzzy SPS (20) can be achieved if there exist positive-definite matrices $\Psi_t = \operatorname{diag}\{\Psi_{1t}, \Psi_{2t}, \Psi_{3t}\}$ and $Y = \operatorname{diag}\{Y_t, Y_t, I, Y_t, Y_t\}\,(t = 1, 2, \ldots, U)$, scalars $\nu_1 > 0$ and $\nu_2 > 0$, and matrices H_{ijt} and $Z_{ijt}(i, j = 1, 2, \ldots, r)$ with compatible dimensions, such that the following LMIs hold:

$$\begin{bmatrix} -\nu_1 I & * \\ QG & -Q \end{bmatrix} \le 0 \quad (36)$$

$$\begin{bmatrix} -\nu_2 I & * \\ QGB_i & -Q \end{bmatrix} \le 0 \quad (37)$$

$$\begin{bmatrix} -\Psi_t & * & * & * & * & * & * \\ 0 & \Lambda_1 & * & * & * & * & * \\ \tilde{\mathcal{F}}_{ijt\bar{\varepsilon}} & \tilde{\mathcal{E}}_{1ijt} & \mathcal{P}_h & * & * & * & * \\ 0 & \tilde{\mathcal{E}}_{2ijt} & 0 & \mathcal{P}_h & * & * & * \\ \Pi_{1i\bar{\varepsilon}} & \Pi_{2i} & 0 & 0 & \Lambda_2 & * & * \\ \tilde{\mathcal{N}}_{1ijt\bar{\varepsilon}}^{a} & \tilde{\mathcal{N}}_{1ijt}^{b} & 0 & 0 & 0 & \mathcal{V} & * \\ 0 & \tilde{\mathcal{N}}_{2ijt}^{b} & 0 & 0 & 0 & 0 & \mathcal{V} \end{bmatrix} < 0 \quad (38)$$

with $L_{j,t} = \bar{Y}_{ti}^{-1}Z_{ijt}$ and $K_{j,t} = \bar{Y}_{ti}^{-1}X_{ijt}$, where

$$\tilde{\mathcal{F}}_{ijt\bar{\varepsilon}} = \begin{bmatrix} \tilde{\mathcal{T}}_{1ijt}E_{\bar{\varepsilon}} & 0 & 0 \\ \tilde{\mathcal{T}}_{2ijt}C_iE_{\bar{\varepsilon}} & \tilde{\mathcal{T}}_{3ijt}E_{\bar{\varepsilon}} & \tilde{\mathcal{T}}_{4ijt} \\ Y_t\Phi_tC_iE_{\bar{\varepsilon}} & Y_t\Phi_tC_iE_{\bar{\varepsilon}} & Y_t\bar{\Phi}_t \end{bmatrix}$$

$$\tilde{\mathcal{E}}_{1ijt} = \begin{bmatrix} 0 & 0 & 0 \\ Y_tD_i - \tilde{\mathcal{T}}_{5ijt}F_i & \tilde{\mathcal{T}}_{5ijt} & -\bar{\alpha}\tilde{\mathcal{T}}_{5ijt} \\ Y_t\Phi_tF_i & -Y_t\Phi_t & \bar{\alpha}Y_t\Phi_t \end{bmatrix}$$

$$\Pi_{1i\bar{\varepsilon}} = \begin{bmatrix} MC_1E_{\bar{\varepsilon}} & MC_1E_{\bar{\varepsilon}} & 0 \\ C_iE_{\bar{\varepsilon}} & C_iE_{\bar{\varepsilon}} & 0 \\ H_iE_{\bar{\varepsilon}} & H_iE_{\bar{\varepsilon}} & 0 \end{bmatrix}$$

$$\Pi_{2i} = \begin{bmatrix} MF_i & -N & 0 \\ F_i & 0 & 0 \\ 0 & 0 & 0 \end{bmatrix}$$

$$\tilde{\mathcal{N}}_{1ijt\bar{\varepsilon}}^{a} = \sqrt{2}\left[\tilde{\mathcal{T}}_{5ijt}\bar{\Upsilon}_2 \;\; \tilde{\mathcal{T}}_{5ijt}\bar{\Upsilon}_2 \;\; B_iZ_{ijt}\bar{\Phi}_t\right]$$

$$\tilde{\mathcal{N}}_{1ijt}^{b} = \sqrt{2}\left[\tilde{\mathcal{T}}_{5ijt}F_i \;\; -\tilde{\mathcal{T}}_{5ijt} \;\; \bar{\alpha}\tilde{\mathcal{T}}_{5ijt}\right]$$

$$\tilde{\mathcal{N}}_{2ijt}^{b} = \sqrt{2}\left[0 \;\; 0 \;\; \sqrt{\bar{\alpha}\vec{\alpha}}\tilde{\mathcal{T}}_{5ijt}\right]$$

$$\tilde{\mathcal{T}}_{1ijt} = Y_tA_i + B_iX_{ijt} - B_iZ_{ijt}C_i, \quad \tilde{\mathcal{T}}_{2ijt} = B_iZ_{ijt}\bar{\Phi}_t$$

$$\tilde{\mathcal{T}}_{3ijt} = Y_tA_i - B_iZ_{ijt}\Phi_tC_i, \quad \tilde{\mathcal{T}}_{4ijt} = -B_iZ_{ijt}\bar{\Phi}_t$$

$$\tilde{\mathcal{T}}_{5ijt} = B_iZ_{ijt}\Phi_t, \quad \tilde{\mathcal{E}}_{2ijt} = \begin{bmatrix} 0 & 0 & \tilde{\mathcal{D}}_{ijt} \end{bmatrix}, \quad \bar{\Upsilon}_2 = C_iE_{\bar{\varepsilon}}$$

$$\tilde{\mathcal{D}}_{ijt} = \begin{bmatrix} 0 & -\sqrt{\bar{\alpha}\vec{\alpha}}(B_iZ_{ijt}\Phi_t)^{\mathrm{T}} & \sqrt{\bar{\alpha}\vec{\alpha}}\Phi_t^{\mathrm{T}}Y_t^{\mathrm{T}} \end{bmatrix}^{\mathrm{T}}$$

$$\Lambda_1 = \operatorname{diag}\{-\gamma^2 I, -I, -I\}$$

$$\Lambda_2 = \text{diag}\left\{-I, -\frac{1}{\psi_3}I, -I\right\}$$
$$\mathcal{P}_h = \text{diag}\{\Psi_{1h} - \mathcal{H}_e\{Y_t\}, \Psi_{2h} - \mathcal{H}_e\{Y_t\},\ \Psi_{3h} - \mathcal{H}_e\{Y_t\}\}$$
$$\mathcal{V} = \text{diag}\{\nu_1 I - \mathcal{H}_e\{Y_t\}\},\quad \mathcal{H}_e\{Y_t\} = Y_t + Y_t^{\mathrm{T}}.$$

Proof: First, according to Schur complement, it is easily observed that (27) and (28) can be guaranteed by (36) and (37), respectively. Then, we rewrite (29) as

$$\mathcal{G}_{ijt\varepsilon} + \mathcal{H}_t < 0 \tag{39}$$

where

$$\mathcal{G}_{ijt\varepsilon} = \mathcal{Q}_{ijt\varepsilon} + 2\nu_1\left(\mathcal{N}_{1ijt\varepsilon}^{\mathrm{T}}\mathcal{N}_{1ijt\varepsilon} + \bar{\mathcal{N}}_{2ijt}^{\mathrm{T}}\bar{\mathcal{N}}_{2ijt}\right)$$
$$\mathcal{Q}_{ijt\varepsilon} = \begin{bmatrix}\Gamma_{1ijt\varepsilon} + \mathcal{A}_1 + \mathcal{B} & * \\ \Gamma_{2ijt\varepsilon} + \mathcal{A}_2 & \Gamma_{3ijt} + \bar{\mathcal{A}}_3\end{bmatrix}$$
$$\bar{\mathcal{A}}_3 = \begin{bmatrix}F_i^{\mathrm{T}}\Theta_1 F_i & * & * \\ -M^{\mathrm{T}}MF_i & M^{\mathrm{T}}M & * \\ 0 & 0 & 0\end{bmatrix}$$
$$\mathcal{H}_t = \text{diag}\left\{-\Psi_{1t}, -\Psi_{2t}, -\Psi_{3t}, -\gamma^2 I, -I, -I\right\}.$$

It is apparently that $\mathcal{H}_t < 0$, and thus, the following ε-independent condition (40) can be derived from (39) by recurring to Lemma 2:

$$\mathcal{G}_{ijt\bar{\varepsilon}} + \mathcal{H}_t < 0. \tag{40}$$

Based on (40), we can get

$$\mathbb{X}_{ijt\bar{\varepsilon}} + 2\nu_1\left(\mathcal{N}_{1ijt\bar{\varepsilon}}^{\mathrm{T}}\mathcal{N}_{1ijt\bar{\varepsilon}} + \bar{\mathcal{N}}_{2ijt}^{\mathrm{T}}\bar{\mathcal{N}}_{2ijt}\right) < 0. \tag{41}$$

Then, by using Schur complement, it can be found that (41) holds if and only if

$$\begin{bmatrix}-\Psi_t & * & * & * & * & * & * \\ 0 & \Lambda_1 & * & * & * & * & * \\ \mathcal{F}_{ijt\bar{\varepsilon}} & \mathcal{E}_{1ijt} & -\Psi_h^{-1} & * & * & * & * \\ 0 & \bar{\mathcal{E}}_{2ijt} & 0 & -\Psi_h^{-1} & * & * & * \\ \Pi_{1i\bar{\varepsilon}} & \Pi_{2i} & 0 & 0 & \Lambda_2 & * & * \\ \mathcal{N}_{1ijt\bar{\varepsilon}}^a & \mathcal{N}_{1ijt}^b & 0 & 0 & 0 & -\frac{1}{\nu_1}I & * \\ 0 & \bar{\mathcal{N}}_{2ijt}^b & 0 & 0 & 0 & 0 & -\frac{1}{\nu_1}I\end{bmatrix} < 0 \tag{42}$$

is satisfied, where

$$\mathcal{N}_{1ijt\bar{\varepsilon}}^a = \sqrt{2}\begin{bmatrix}\Upsilon_1\bar{\Upsilon}_2 & \Upsilon_1\bar{\Upsilon}_2 & B_i L_{j,t}\bar{\Phi}_t\end{bmatrix}$$
$$\mathcal{N}_{1ijt}^b = \sqrt{2}\begin{bmatrix}\Upsilon_1 F_i & -\Upsilon_1 & \bar{\alpha}\Upsilon_1\end{bmatrix}$$
$$\bar{\mathcal{N}}_{2ijt}^b = \sqrt{2}\begin{bmatrix}0 & 0 & \sqrt{\bar{\alpha}\bar{\alpha}}\Upsilon_1\end{bmatrix}.$$

By further premultiplying and postmultiplying the left-hand side of (42) with $\text{diag}\{I, I, Y\}$ and $\text{diag}\{I, I, Y^{\mathrm{T}}\}$, respectively, it has

$$\begin{bmatrix}\Xi_{1t} & * & * \\ \Xi_{2ijt\bar{\varepsilon}} & \Xi_{3h} & * \\ \Xi_{4ijt\bar{\varepsilon}} & 0 & \Xi_5\end{bmatrix} < 0 \tag{43}$$

where

$$\Xi_{1t} = \begin{bmatrix}-\Psi_t & * \\ 0 & \Lambda_1\end{bmatrix},\quad \Xi_{2ijt\bar{\varepsilon}} = \begin{bmatrix}Y_t\mathcal{F}_{ijt\bar{\varepsilon}} & Y_t\mathcal{E}_{1ijt} \\ 0 & Y_t\bar{\mathcal{E}}_{2ijt}\end{bmatrix}$$
$$\Xi_{3h} = \text{diag}\left\{-Y_t\Psi_h^{-1}Y_t^{\mathrm{T}}, -Y_t\Psi_h^{-1}Y_t^{\mathrm{T}}\right\}$$
$$\Xi_{4ijt\bar{\varepsilon}} = \begin{bmatrix}\Pi_{1i\bar{\varepsilon}} & \Pi_{2i} \\ Y_t\mathcal{N}_{1ijt\bar{\varepsilon}}^a & Y_t\mathcal{N}_{1ijt}^b \\ 0 & Y_t\bar{\mathcal{N}}_{2ijt}^b\end{bmatrix}$$
$$\Xi_5 = \text{diag}\left\{\Lambda_2, -Y_t\frac{1}{\nu_1}IY_t^{\mathrm{T}}, -Y_t\frac{1}{\nu_1}IY_t^{\mathrm{T}}\right\}.$$

For positive-definite matrices $\Psi_h = \text{diag}\{\Psi_{1h}, \Psi_{2h}, \Psi_{3h}\}$ with $\Psi_{fh} > 0\,(f = 1, 2, 3)$, it can be known that $\Psi_{fh}^{-1} > 0$. Hence, we can derive that

$$(\Psi_{fh} - Y_t)\Psi_{fh}^{-1}(\Psi_{fh} - Y_t)^{\mathrm{T}} = \Psi_{fh} - Y_t - Y_t^{\mathrm{T}} + Y_t\Psi_{fh}^{-1}Y_t^{\mathrm{T}} \geq 0$$

which is obviously followed by $-Y_t\Psi_{fh}^{-1}Y_t^{\mathrm{T}} \leq \Psi_{fh} - \mathcal{H}_e\{Y_t\}$. According to the similar process, it is not hard to get $-Y_t(1/\nu_1)IY_t^{\mathrm{T}} \leq \nu_1 I - \mathcal{H}_e\{Y_t\}$.

Given that the SVD for B_i with full rank can be expressed as $B_i = O_i\begin{bmatrix}N_i \\ 0\end{bmatrix}V_i$, where $O_i^{\mathrm{T}}O_i = I$ and $V_i^{\mathrm{T}}V_i = I$, thus for $Y_t = O_i\begin{bmatrix}D_{it} & 0 \\ 0 & E_{it}\end{bmatrix}O_i^{\mathrm{T}}$, it can be deduced that $Y_tB_i = B_i\bar{Y}_{ti}$ with $\bar{Y}_{ti} = V_iN_i^{-1}D_{it}N_iV_i^{\mathrm{T}}$ based on Lemma 1. Then, by defining $Z_{ijt} = \bar{Y}_{ti}L_{j,t}$, $X_{ijt} = \bar{Y}_{ti}K_{j,t}$, and substituting $-Y_t\Psi_{fh}^{-1}Y_t^{\mathrm{T}}$ and Y_tB_i in (43) with $\Psi_{fh} - \mathcal{H}_e\{Y_t\}$ and $B_i\bar{Y}_{ti}$, respectively, (38) can be finally derived. Additionally, we can get that $L_{j,t} = \bar{Y}_{ti}^{-1}Z_{ijt}$ and $K_{j,t} = \bar{Y}_{ti}^{-1}X_{ijt}$. Therefore, the proof is accomplished. ■

IV. Dynamic Learning-Based APSO Algorithm for Optimizing the Proposed SMC Method

As revealed by the above analysis, the sliding domain actually refers to the region of the system state governed by the SMC law, and thus, it is crucial to minimize the domain for achieving desirable control performance effectively. In view of this, we dedicate to design a dynamic-learning-based APSO algorithm to optimize the presented SMC method in this section. To be specific, some preliminary knowledge is briefed first, which is followed by the introduction of the proposed algorithm.

A. Preliminary Knowledge

For the APSO algorithm, the candidate solutions to a problem with the fitness function Fit are treated as a swarm of particles, and each particle is depicted by two attributes, i.e., velocity and position. Focusing on the gth particle, the velocity v_g and position p_g will be iteratively updated, and the specific updating principle can be described as follows:

$$v_g^l = \beta^l v_g^{l-1} + c_1\pi_1\left(\text{Pbest}_g^{l-1} - p_g^{l-1}\right) + c_2\pi_2\left(\text{Gbest}^{l-1} - p_g^{l-1}\right) \tag{44}$$
$$p_g^l = p_g^{l-1} + v_g^l \tag{45}$$

where c_1 and c_2 represent the acceleration parameters; π_1 and $\pi_2 \in [0, 1]$ are the two uniformly distributed random numbers; Pbest_g^{l-1} and Gbest^{l-1} denote the local best position of the gth particle and the best position of the entire particle swarm during the first $l-1$ iterations, respectively; β^l is the inertia weight factor, which will decrease from $\beta_{\max}$ to $\beta_{\min}$ according

to the rule $\beta^l = ((\mathbf{U}-l)/\mathbf{U})(\beta_{\max}-\beta_{\min})+\beta_{\min}$, where $\mathbf{U}$ is the maximum number of iterations.

Remark 3: Compared with the traditional PSO algorithm with a fixed inertia weight factor, adaptive β^l is adopted in the described APSO algorithm to enhance the applicability of the algorithm. Moreover, as reflected in (44) and (45), the movement of each particle is only affected by its own Pbest and the Gbest without considering the influence of neighboring particles, which will increase the risk of the algorithm falling into local optimum.

In response to the mentioned risk, a dynamic learning approach was presented in [29] to enable each particle probabilistically learns the optimal information of other particles. The dynamic learning-based updating rule for the velocity v_g and position p_g is

$$v_g^l = \beta^l v_g^{l-1} + c_1\pi_1\left(\text{Pbest}_{\tilde{g}}^{l-1} - p_g^{l-1}\right) + c_2\pi_2\left(\text{Gbest}^{l-1} - p_g^{l-1}\right) \tag{46}$$

$$p_g^l = p_g^{l-1} + v_g^l \tag{47}$$

where $\tilde{g} = \mod(g+\mathbb{P}*\pi_4, S)$ if a random number π_3 satisfies that $\pi_3 \le \mathbf{K}_g^l$; otherwise, $\tilde{g} = g$; $\mathbf{K}_g^l = b_1 + b_2(1/\sqrt{T_g^l})$; b_1 and b_2 are the weighting coefficients within $[0,1]$; T_g^l is the ranking number of the gth particle in lth iteration based on its fitness value, i.e., the value of Fit derived according to p_g^{l-1}; π_4 is a random number lies in $[-1,1]$; S is the total number of particles; and $\mathbb{P}$ is the neighborhood size.

B. Algorithm for Optimizing the Sliding Domain

It can be observed from (30) that the optimization of the sliding domain is closely related to the adjustable parameters ν_2 and Q. Meanwhile, it is worth noting that the selection of $\bar{\varepsilon}$ obviously affects the range of the sliding domain. Hence, we then design a dynamic learning-based APSO algorithm to search the optimal $\bar{\varepsilon}$, ν_2, and Q to minimize the sliding domain. By setting $\text{Fit} = \sqrt{(2\mathbf{d}^2\nu_2/\lambda_{\min}(Q))}$, the formulation of the studied optimization problem can be given as follows:

$$\min_{\bar{\varepsilon},\nu_2,Q} \text{Fit} \quad \text{s.t. the conditions (36)}-\text{(38)}. \tag{48}$$

To solve the formulated problem, we take the combination of $\bar{\varepsilon}$, ν_2, and Q as a particle, and thus, let $p = [\bar{\varepsilon}, \nu_2, Q]$, and the search space is defined as $\mathcal{R} \triangleq \{(v_g, p_g)|v_g \in [\underline{v}_g, \overline{v}_g], p_g \in [\underline{p}_g, \overline{p}_g], g = 1,\ldots,S\}$. The algorithm will be implemented within $\mathbf{U}$ rounds, and in the lth round, for each particle, v_g and p_g are first updated based on the dynamic learning rule depicted by (46) and (47), and then, the fitness is calculated based on the latest p_g (we should note that the feasible solution to the LMIs presented in (36)–(38) may not be found under the p_g, and then, the fitness is set to be a huge value $\mathbf{N}$); if more desirable fitness can be obtained based on the updated p_g, then the local best fitness, denoted by Fit_g, is improved and the corresponding p_g is saved as Pbest_g^l, which is followed by a possible updating of the global best fitness, indicated by Fit^* and Gbest^l. More specific description about the proposed algorithm is given in Algorithm 1. Then, to calculate the observer and controller gains, Algorithm 1 is first conducted to obtain the optimal parameters $\bar{\varepsilon}$, ν_2, and Q, and consequently, LMI tools can be used to solve the LMIs (36)–(38) so as to get the gains $L_{j,t}$ and $K_{j,t}$. By referring to the existed researches [35], [36], the detailed process can be found in Algorithm 2.

Algorithm 1 Dynamic Learning-Based APSO Algorithm for Optimizing the Sliding Domain

```
Given the system parameters A_i, B_i, C_i, D_i, F_i, H_i, G, W; the positive parameters d, ψ_1, ψ_2, γ, ᾱ; the APSO-related scalars b_1, b_2, c_1, c_2, β_max, β_min, U, S, ℙ;
Generating the initial v_g^0 and p_g^0 in the given search space R, setting Pbest_g^0 = Gbest^0 = p_g^0, and initializing the fitness values Fit_g and Fit^*;
for l = 1; l ≤ U; l = l + 1 do
    Gbest^l = Gbest^{l-1};
    for g = 1; g ≤ S; g = g + 1 do
        Pbest_g^l = Pbest_g^{l-1};
        Updating v_g^l and p_g^l based on (46), (47);
        if LMIs (36)-(38) can be solved based on p_g^l then
            calculating the fitness J = sqrt(2d^2 ν_2 / λ_min(Q));
        else
            J = N;
        end
        if J ≤ Fit_g then
            Fit_g = J, Pbest_g^l = P_g^l;
        end
        if Fit_g ≤ Fit^* then
            Fit^* = Fit_g, Gbest^l = Pbest_g^l;
        end
    end
end
```

Algorithm 2 Calculation of the Gains $L_{j,t}$ and $K_{j,t}$

```
Given the system parameters A_i, B_i, C_i, D_i, F_i, H_i, G, W; the positive parameters d, ψ_1, ψ_2, γ, ᾱ; the APSO-related scalars b_1, b_2, c_1, c_2, β_max, β_min, U, S, ℙ;
Obtaining the optimal ε̄, ν_2, and Q via conducting Algorithm 1;
Adopting LMI toolbox in MATLAB to solve LMIs (36)-(38);
while tmin ≥ 0 do
    Adjusting some positive and APSO-related parameters;
    Recomputing the optimal ε̄, ν_2 and Q;
    Resolving LMIs (36)-(38);
end
Using SVD to calculate Ȳ_ti;
L_{j,t} = Ȳ_ti^{-1} Z_ijt, K_{j,t} = Ȳ_ti^{-1} X_ijt.
```

Remark 4: We note that the performance of the proposed SMC method is influenced by some design parameters, such as the parameters about the DETM, i.e., ψ_1 and ψ_2, the upper-bound of the SPP $\bar{\varepsilon}$, and the positive scalars ν_1, ν_2, and Q. For ψ_1 (ψ_2), it can be observed from (3) and (4) that the smaller the value of it, the more likely the event-triggering condition can be satisfied. With more released data, the improved SMC performance can be expected. However, ψ_1 (ψ_2) should not be arbitrarily small as further reduction will increase network traffic load. For $\bar{\varepsilon}$, it is generally acknowledged that a smaller $\bar{\varepsilon}$ typically leads to faster convergence of the system to the sliding surface, which resulting in improved SMC performance. For the positive parameters ν_1, ν_2, and Q, it is challenging to identify clear patterns in their influence on the

SMC performance. To address this, Algorithm 1 with the aim $\min_{\bar{\varepsilon},\nu_2,Q}$ Fit is presented to optimize the SMC performance.

Remark 5: While the integration of the proposed DETM, MWTOD protocol, and dynamic learning-based APSO algorithm enhances the performance of the SMC approach in complex environments, it is important to note that this incorporation may introduce increased system complexity. Fortunately, this challenge can be mitigated by leveraging technologies such as edge/cloud computing, parallel computing, and software-defined networking, which can help manage and reduce complexity, thereby ensuring that the proposed SMC method remains feasible for real-time applications.

Remark 6: In this work, the SMC problem for fuzzy SPSs subject to FDI attacks and communication constraints is studied comprehensively. In contrast to the existing research, which either uses DETM [19], [20] or WTOD protocol [13], [14] individually to address the communication constraints of fuzzy SPSs, this study integrates the proposed DETM and MWTOD protocol to achieve enhanced bandwidth adaptability and utilization. Although the combined DETM and WTOD framework has been explored in [37], this study takes multichannel communication into consideration so as to provide a more practical solution. To cope with FDI attacks, secure SMC methods for various systems have been reported in the literature [25], [38]; however, this work considers a more complicated scenario where the system is driven by nonlinearities and exhibits a two-timescale feature. Furthermore, this study achieves the optimal SMC performance via a dynamic learning technique, which is unexplored in [25] and [38]. Comparing with [34], which also employs the APSO algorithm to enhance the SMC performance for fuzzy SPSs, this article introduces the SPP as an optimization factor to further improve the system's robustness in managing two-timescale dynamics.

V. Numerical Results

In this section, we conduct simulations over a PC platform (CPU: i7-12700 2.10 GHz and memory: 32G) deployed with MATLAB R2024a to demonstrate the feasibility of the proposed SMC scheme. Specifically, we consider the F-404 aircraft engine system introduced in [39]. For the system, three sensors are assumed to acquire the system state (i.e., $n_y = 3$), which is set as $x(k) = \begin{bmatrix} x_1(k) & x_2(k) & x_3(k) \end{bmatrix}^{\mathrm{T}}$ with $n_s = 1$ and $n_f = 2$, where $x_1(k)$, $x_2(k)$, and $x_3(k)$ represent the sideslip angle, roll rate, and yaw rate, respectively. The system matrices $A_i (i = 1, 2)$ are defined as

$$A_i = \begin{bmatrix} -1.46 & 0 & 2.428 \\ 0.1643 + 0.5\delta_i & -0.4 + \delta_i & -0.3788 \\ 0.3107 & 0 & -2.23 \end{bmatrix} \quad (49)$$

with $\delta_1 = -0.5$ and $\delta_2 = -1$ [39]. The other model parameters are set as

$$B_1 = \begin{bmatrix} -0.1512 & -0.0214 & 0.1052 \\ -0.3219 & -0.1154 & 0.0945 \\ 0.0311 & 0.1652 & 0.1074 \end{bmatrix}$$

$$B_2 = \begin{bmatrix} 0.1599 & -0.1321 & 0.0251 \\ -0.1009 & -0.1234 & 0.1898 \\ 0.0225 & 0.1241 & -0.1149 \end{bmatrix}$$

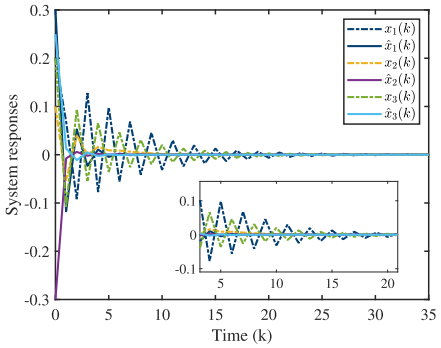

Fig. 2. System state $x(k)$ and observed state $\hat{x}(k)$.

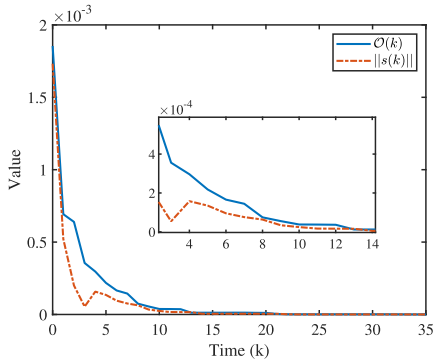

Fig. 3. Sliding domain $\mathcal{O}(k)$ and $\|s(k)\|$.

TABLE I
Data Transmission Ratio Under Different ψ_1

The value of ψ_1	The data transmission ratio
case1: ψ_1=0.75	34.3%
case2: ψ_1=0.45	51.4%
case3: ψ_1=0.10	60.0%

$$C_1 = \mathrm{diag}\{0.18, 0.12, 0.17\}, \quad C_2 = \mathrm{diag}\{0.17, 0.15, 0.19\}$$
$$H_1 = \mathrm{diag}\{0.08, 0.12, 0.18\}, \quad H_2 = \mathrm{diag}\{0.2, 0.1, 0.17\}$$
$$D_1 = \mathrm{diag}\{0.5, 0.5, 0.5\}, \quad D_2 = \mathrm{diag}\{0.5, 0.5, 0.5\}$$
$$F_1 = \mathrm{diag}\{-0.1, 0.1, 0.1\}, \quad F_2 = \mathrm{diag}\{-0.15, 0.12, -0.19\}$$
$$G = \mathrm{diag}\{0.1, 0.5, 0.4\}, \quad W = \mathrm{diag}\{0.1, 0.3, 0.25\}.$$

The fuzzy membership functions are chosen as

$$v_1(\mu(k)) = \frac{1 - sin^2(\|x_1(k)\|_2)}{2}, \quad v_2(\mu(k)) = 1 - v_1(\mu(k)).$$

The number of available channels is supposed to be $n = 2$, and then, it can be derived that $U = 3$. By setting the scalars $\psi_1 = 0.15, \psi_2 = 0.45, \rho = 1, \gamma = 1, \mathbf{d} = 0.1$, and $\bar{\alpha} = 0.4$, and the proposed APSO-related parameters $\mathbf{U} = 150$, $S = 50$, $b_1 = 0.1$, $b_2 = 0.4$, $c_1 = c_2 = 2$, $\beta_{\max} = 0.9$, $\beta_{\min} = 0.4$, $\mathbb{P} = 8$, $\mathcal{R} = \{(v_g, p_g)|v_g \in [-0.5, 0.5], \bar{\varepsilon} \in [0, 0.4], \nu_2 \in [0.5, 3.5]$, and $Q \in [0.1, 4.5]\}$, Algorithm 2 is then applied to obtain the observer and controller gains.

Based on initializing $x(0) = \begin{bmatrix} 0.2 & 0.1 & 0.2 \end{bmatrix}^{\mathrm{T}}$ and $\hat{x}(0) = \begin{bmatrix} 0.3 & -0.3 & 0.25 \end{bmatrix}^{\mathrm{T}}$, the final simulation results are presented in Figs. 2–7 and Tables I–III. Specifically, the system state and its estimation are shown in Fig. 2; it can be found that the observed state is gradually closing to the real system

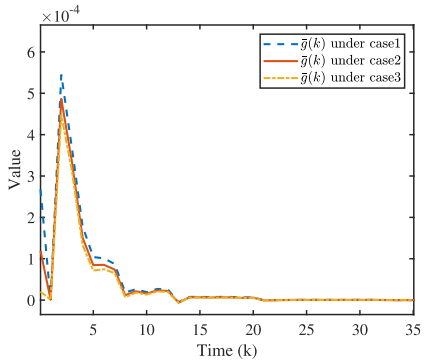

Fig. 4. Trajectories of $\bar{g}(k)$ under different values of ψ_1.

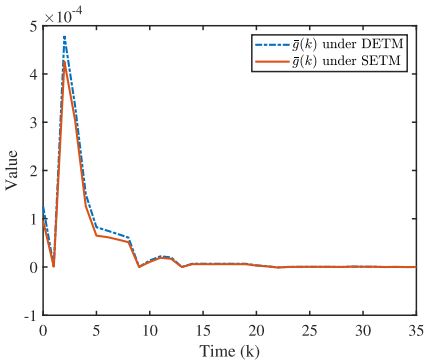

Fig. 5. Trajectories of $\bar{g}(k)$ under the DETM and SETM.

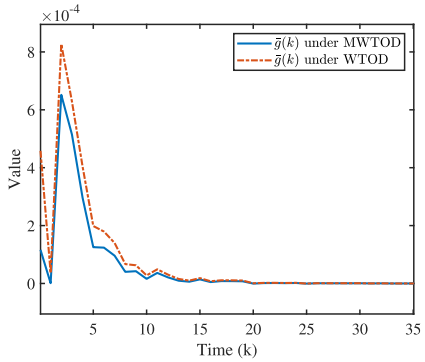

Fig. 6. Trajectories of $\bar{g}(k)$ under the MWTOD and WTOD protocols.

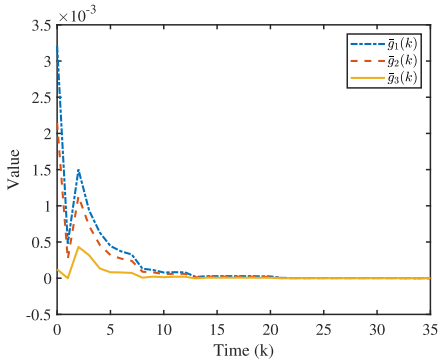

Fig. 7. Trajectories of $\bar{g}_1(k)$, $\bar{g}_2(k)$, and $\bar{g}_3(k)$.

state, which validates the efficiency of the devised observer; furthermore, the system state converges to 0 within about 20 time instants, which confirms that the stability of the considered system can be guaranteed with the designed sliding mode controller. The sliding domain $\mathcal{O}(k)$ obtained based on the presented APSO algorithm and the corresponding $\|s(k)\|$ are shown in Fig. 3; we observe that the reachability of the sliding surface for the T–S fuzzy SPS can be achieved; thus, the effectiveness of the proposed controller can be further verified.

TABLE II
AMOUNT OF DATA TRANSMISSION

Performance metrics	DETM	SETM ($\psi(k) = \psi_1$)
The number of transmitted packets	20	28
The data transmission ratio	57.1%	80.0%

TABLE III
MEAN AND VARIANCE OF SIDESLIP ANGLE UNDER DIFFERENT ATTACK PROBABILITIES

Attack probability	Sideslip angle mean	Sideslip angle variance
$\bar{\alpha}$=0.2	0.01511	0.00395
$\bar{\alpha}$=0.5	0.01619	0.00413
$\bar{\alpha}$=0.8	0.01714	0.00457

The presented SMC performance is achieved within the communication constraints, which critically rely on the designed DETM. It can be observed from (3) and (4) that the smaller the value of $\psi_1(\psi_2)$, the more likely the event-triggering condition can be satisfied. Table I shows the data transmission ratio under three cases, and it confirms that a reduction in ψ_1 leads to an increase in data release. With more released data, the improved SMC performance can be expected. Therefore, we then define $\bar{g}(k) = \mathcal{O}(k) - \|s(k)\|$ as a performance metric and compare the values of $\bar{g}(k)$ obtained under the three cases. As verified in Fig. 4, the smallest $\bar{g}(k)$ is achieved under case3, where 60.0% data packets are released with $\psi_1 = 0.10$ (the similar results can also be obtained with different values of ψ_2). However, it is important to note that $\psi_1(\psi_2)$ should not be arbitrarily small, as further reduction will significantly increase network traffic load.

Moreover, by setting $\psi(k) = \psi_1$, the DETM is reduced to a traditional SETM. Then, Table II illustrates the amount of data transmission under both the DETM and SETM. It can be found that the DETM results in lower data transmission compared to the SETM, which indicates a more efficient reduction in network traffic load. Furthermore, as shown in Fig. 5, the reduction in data transmission achieved by the DETM did not cause a significant increase in $\bar{g}(k)$ compared with the SETM. This demonstrates that the proposed DETM-based SMC method effectively balances the mitigation of data traffic with the enhancement of control performance.

Besides the DETM, the MWTOD protocol is also designed to avoid data collision as well as improve channel utilization. Thus, we then compare the SMC performance under the MWTOD protocol with that of the traditional WTOD protocol. As shown in Fig. 6, $\bar{g}(k)$ obtained under the proposed MWTOD protocol is smaller than that derived under the traditional WTOD protocol. The reason is that the MWTOD protocol fully utilizes the available communication channels,

which allows more measurement signals to be transmitted, thereby improving the SMC performance.

Considering the stochastic feature of the FDI attacks, we further conduct simulations based on multiple Monte Carlo runs to analyze the mean and variance of the system sideslip angle. As revealed by Table III, both the mean and variance of the sideslip angle increase with rising attack probability, which indicates that higher attack probability leads to greater system instability. Meanwhile, the results also validate the significance of the designed SMC method in maintaining the performance of fuzzy SPSs under such attacks.

Finally, to demonstrate the efficiency of the proposed dynamic learning-based APSO algorithm, we use $\bar{g}_1(k)$, $\bar{g}_2(k)$, and $\bar{g}_3(k)$ to denote $\bar{g}(k)$ obtained without optimization, under the traditional PSO algorithm [40] and under our designed algorithm, respectively, and display the trajectories of them in Fig. 7. As shown, $\bar{g}_3(k)$ is smaller than both $\bar{g}_1(k)$ and $\bar{g}_2(k)$, which reveals the superiority of the devised algorithm.

VI. Conclusion

In this article, under the scenario that the multichannel-enabled communication network is hindered by limited bandwidth and FDI attacks, the dynamic learning-based optimal SMC method has been proposed for T–S fuzzy SPSs. To be specific, to overcome the bandwidth limitations, the DETM and MWTOD protocols have been introduced, which have not only reduced the network traffic load but also ensured collision-free data transmission and full channel utilization. FDI attacks have been modeled using a Bernoulli process, and an augmented model of the T–S fuzzy SPS with an observer-based sliding mode controller has been developed. Then, the approach for designing the observer and controller gain matrices has been reported based on the stability and reachability analysis of the formulated system. Furthermore, the dynamic learning-based APSO algorithm has been designed to achieve the optimal SMC performance. The simulation results have been finally presented to demonstrate the effectiveness of the proposed SMC method. We should clarify that the proposed SMC approach is based on certain underlying constraints, i.e., the precise knowledge of the available channels, probability and energy upper bound of the attacks, and system dynamics. In the future, we will focus on developing methods to relax these constraints so as to provide a more practical SMC method. Additionally, we will explore more complex attack scenarios to further enhance the robustness of the system.

References

[1] B. Zhao, G. Shi, and D. Liu, "Event-triggered local control for nonlinear interconnected systems through particle swarm optimization-based adaptive dynamic programming," *IEEE Trans. Syst., Man, Cybern., Syst.*, vol. 53, no. 12, pp. 7342–7353, Dec. 2023.

[2] W. Ren, B. Jiang, and H. Yang, "Fault-tolerant control of singularly perturbed systems with applications to hypersonic vehicles," *IEEE Trans. Aerosp. Electron. Syst.*, vol. 55, no. 6, pp. 3003–3015, Dec. 2019.

[3] X. Jin, J. Qin, W. X. Zheng, and C. Yang, "Adaptive perturbation rejection control for a class of converter systems with circuit realization," *IEEE Trans. Syst., Man, Cybern., Syst.*, vol. 52, no. 8, pp. 4740–4750, Aug. 2022.

[4] Y. Zhou et al., "Distributed motion control for multiple mobile robots using discrete-event systems and model predictive control," *IEEE Trans. Syst., Man, Cybern., Syst.*, vol. 54, no. 2, pp. 997–1010, Feb. 2024.

[5] J. Wang, Z. Huang, Z. Wu, J. Cao, and H. Shen, "Extended dissipative control for singularly perturbed PDT switched systems and its application," *IEEE Trans. Circuits Syst. I, Reg. Papers*, vol. 67, no. 12, pp. 5281–5289, Dec. 2020.

[6] X. Wan, T. Han, J. An, and M. Wu, "Hidden Markov model based fault detection for networked singularly perturbed systems," *IEEE Trans. Syst., Man, Cybern., Syst.*, vol. 51, no. 10, pp. 6445–6456, Oct. 2021.

[7] J. Cheng, Y. Wang, J. H. Park, J. Cao, and K. Shi, "Static output feedback quantized control for fuzzy Markovian switching singularly perturbed systems with deception attacks," *IEEE Trans. Fuzzy Syst.*, vol. 30, no. 4, pp. 1036–1047, Apr. 2022.

[8] J. Xu, Y. Niu, and H.-K. Lam, "Nonperiodic multirate sampled-data fuzzy control of singularly perturbed nonlinear systems," *IEEE Trans. Fuzzy Syst.*, vol. 31, no. 9, pp. 2891–2903, Sep. 2023.

[9] J. Li, J. Wang, H. Peng, Y. Hu, and H. Su, "Fuzzy-torque approximation-enhanced sliding mode control for lateral stability of mobile robot," *IEEE Trans. Syst., Man, Cybern., Syst.*, vol. 52, no. 4, pp. 2491–2500, Apr. 2022.

[10] Y. Wang, X. Xie, M. Chadli, S. Xie, and Y. Peng, "Sliding-mode control of fuzzy singularly perturbed descriptor systems," *IEEE Trans. Fuzzy Syst.*, vol. 29, no. 8, pp. 2349–2360, Aug. 2021.

[11] S. Ding, Q. Hou, and H. Wang, "Disturbance-observer-based second-order sliding mode controller for speed control of PMSM drives," *IEEE Trans. Energy Convers.*, vol. 38, no. 1, pp. 100–110, Mar. 2023.

[12] F. Wang, J. Liang, J. Lam, J. Yang, and C. Zhao, "Robust filtering for 2-D systems with uncertain-variance noises and weighted try-once-discard protocols," *IEEE Trans. Syst., Man, Cybern., Syst.*, vol. 53, no. 5, pp. 2914–2924, May 2023.

[13] J. Wang, C. Yang, J. Xia, Z.-G. Wu, and H. Shen, "Observer-based sliding mode control for networked fuzzy singularly perturbed systems under weighted try-once-discard protocol," *IEEE Trans. Fuzzy Syst.*, vol. 30, no. 6, pp. 1889–1899, Jun. 2022.

[14] Y. Hu, C. Cai, H. Lin, and O.-M. Kwon, "Fuzzy-model-based H_∞ control for networked singularly perturbed systems: The asynchronous weighted try-once-discard protocol case," *IEEE Trans. Fuzzy Syst.*, vol. 32, no. 5, pp. 2713–2724, May 2024.

[15] C. Knill, F. Embacher, B. Schweizer, S. Stephany, and C. Waldschmidt, "Coded OFDM waveforms for MIMO radars," *IEEE Trans. Veh. Technol.*, vol. 70, no. 9, pp. 8769–8780, Sep. 2021.

[16] W. Li et al., "A portable and a scalable multi-channel wireless recording system for wearable electromyometrial imaging," *IEEE Trans. Biomed. Circuits Syst.*, vol. 17, no. 5, pp. 916–927, Oct. 2023.

[17] Y. Fan, Y. Wu, J. Yuan, J. Gao, and H. Qiao, "Event-triggered sliding-mode control for a discrete-time muscle-driven musculoskeletal system," *IEEE Trans. Autom. Sci. Eng.*, vol. 21, no. 4, pp. 5866–5880, Oct. 2024.

[18] D. Yao, H. Li, and Y. Shi, "Event-based average consensus of disturbed MASs via fully distributed sliding mode control," *IEEE Trans. Autom. Control*, vol. 69, no. 3, pp. 2015–2022, Mar. 2024.

[19] W. Qi, C. Zhang, G. Zong, S.-F. Su, and M. Chadli, "Finite-time event-triggered stabilization for discrete-time fuzzy Markov jump singularly perturbed systems," *IEEE Trans. Cybern.*, vol. 53, no. 7, pp. 4511–4520, Jul. 2023.

[20] H. Shen, Y.-A. Liu, J. Wang, H. Yan, and M. Chadli, "Sliding-mode control for IT2 fuzzy nonlinear singularly perturbed systems and its application to electric circuits: A dynamic event-triggered mechanism," *IEEE Trans. Syst., Man, Cybern., Syst.*, vol. 53, no. 7, pp. 4077–4090, Jul. 2023.

[21] J. Cheng, J. H. Park, H. Yan, and Z.-G. Wu, "An event-triggered round-robin protocol to dynamic output feedback control for nonhomogeneous Markov switching systems," *Automatica*, vol. 145, Nov. 2022, Art. no. 110525.

[22] J. Liu, J. Ke, J. Liu, X. Xie, and E. Tian, "Outlier-resistant non-fragile control of nonlinear networked systems under DoS attacks and multi-variable event-triggered SC protocol," *IEEE Trans. Inf. Forensics Security*, vol. 19, pp. 2609–2622, 2024.

[23] Q. Zhang and D. He, "Adaptive neural control of nonlinear cyber–physical systems against randomly occurring false data injection attacks," *IEEE Trans. Syst., Man, Cybern., Syst.*, vol. 53, no. 4, pp. 2444–2455, Apr. 2023.

[24] M. Li and Y. Chen, "Wide-area robust sliding mode controller for power systems with false data injection attacks," *IEEE Trans. Smart Grid*, vol. 11, no. 2, pp. 922–930, Mar. 2020.

[25] M. Li, Y. Chen, Y. Zhang, and Y. Liu, "Adaptive sliding-mode tracking control of networked control systems with false data injection attacks," *Inf. Sci.*, vol. 585, pp. 194–208, Mar. 2022.

[26] J. Song, Y. Niu, H.-K. Lam, and Y. Zou, "Asynchronous sliding mode control of singularly perturbed semi-Markovian jump systems: Application to an operational amplifier circuit," *Automatica*, vol. 118, Aug. 2020, Art. no. 109026.
[27] M. Navabi, A. Davoodi, and M. Reyhanoglu, "Optimum fuzzy sliding mode control of fuel sloshing in a spacecraft using PSO algorithm," *Acta Astronautica*, vol. 167, pp. 331–342, Feb. 2020.
[28] F. F. M. El-Sousy, M. M. Amin, and O. A. Mohammed, "Robust adaptive neural network tracking control with optimized super-twisting sliding-mode technique for induction motor drive system," *IEEE Trans. Ind. Appl.*, vol. 58, no. 3, pp. 4134–4157, May 2022.
[29] Z.-H. Liu, H.-L. Wei, X.-H. Li, K. Liu, and Q.-C. Zhong, "Global identification of electrical and mechanical parameters in PMSM drive based on dynamic self-learning PSO," *IEEE Trans. Power Electron.*, vol. 33, no. 12, pp. 10858–10871, Dec. 2018.
[30] C. Du, Z. Yin, Y. Zhang, J. Liu, X. Sun, and Y. Zhong, "Research on active disturbance rejection control with parameter autotune mechanism for induction motors based on adaptive particle swarm optimization algorithm with dynamic inertia weight," *IEEE Trans. Power Electron.*, vol. 34, no. 3, pp. 2841–2855, Mar. 2019.
[31] H. Shen, Y. Men, Z. Wu, and J. H. Park, "Nonfragile H_∞ control for fuzzy Markovian jump systems under fast sampling singular perturbation," *IEEE Trans. Syst., Man, Cybern., Syst.*, vol. 48, no. 12, pp. 2058–2069, Dec. 2018.
[32] J. Wang, C. Yang, H. Shen, J. Cao, and L. Rutkowski, "Sliding-mode control for slow-sampling singularly perturbed systems subject to Markov jump parameters," *IEEE Trans. Syst., Man, Cybern., Syst.*, vol. 51, no. 12, pp. 7579–7586, Dec. 2021.
[33] L. Zha, R. Liao, J. Liu, X. Xie, E. Tian, and J. Cao, "Dynamic event-triggered output feedback control for networked systems subject to multiple cyber attacks," *IEEE Trans. Cybern.*, vol. 52, no. 12, pp. 13800–13808, Dec. 2022.
[34] Y. Yang, Y. Niu, and H. Reza Karimi, "Dynamic learning control design for interval type-2 fuzzy singularly perturbed systems: A component-based event-triggering protocol," *Int. J. Robust Nonlinear Control*, vol. 32, no. 5, pp. 2518–2535, Mar. 2022.
[35] H. Shen, C. Peng, H. Yan, and S. Xu, "Data-driven near optimization for fast sampling singularly perturbed systems," *IEEE Trans. Autom. Control*, vol. 69, no. 7, pp. 4689–4694, Jul. 2024.
[36] J. Wang, Y. Huang, X. Xie, H. Yan, and H. Shen, "Optimal control for fuzzy Markov jump singularly perturbed systems: A hybrid zero-sum game iteration approach," *IEEE Trans. Fuzzy Syst.*, vol. 32, no. 11, pp. 6388–6398, Nov. 2024.
[37] J. Liu, E. Gong, L. Zha, E. Tian, and X. Xie, "Interval type-2 fuzzy-model-based filtering for nonlinear systems with event-triggering weighted try-once-discard protocol and cyberattacks," *IEEE Trans. Fuzzy Syst.*, vol. 32, no. 3, pp. 721–732, Mar. 2024.
[38] W. Guo, F. Liu, Y. Wang, D. Sidorov, and J. Wu, "Adaptive event-triggered sliding mode load frequency control for cyber-physical power systems under false data injection attacks," *IEEE Trans. Ind. Informat.*, vol. 21, no. 4, pp. 2947–2956, Apr. 2025.
[39] S. Fu, J. Qiu, L. Chen, and M. Chadli, "Adaptive fuzzy observer-based fault estimation for a class of nonlinear stochastic hybrid systems," *IEEE Trans. Fuzzy Syst.*, vol. 30, no. 1, pp. 39–51, Jan. 2022.
[40] A. Godio and A. Santilano, "On the optimization of electromagnetic geophysical data: Application of the PSO algorithm," *J. Appl. Geophysics*, vol. 148, pp. 163–174, Jan. 2018.

Yan Li received the dual Ph.D. degree in computer science from the University of Science and Technology of China, Hefei, China, and the City University of Hong Kong, Hong Kong, in 2011.

She is currently an Associate Professor with the School of Computer and Artificial Intelligence, Nanjing University of Finance and Economics, Nanjing, China. Her research interests include networked control systems, learning-based algorithms, and software-defined networking.

Ding Zhu received the M.Sc. degree in software engineering from the School of Computer and Artificial Intelligence, Nanjing University of Finance and Economics, Nanjing, China, in 2025.

His research interests include fuzzy systems, robust control, and state estimation.

Lijuan Zha received the Ph.D. degree in control science and engineering from Donghua University, Shanghai, China, in 2018.

From December 2017 to March 2024, she was an Associate Professor with the College of Information and Engineering, Nanjing University of Finance and Economics, Nanjing, China. Since April 2024, she has been a Professor with the College of Science, Nanjing Forestry University, Nanjing. Her research interests include networked control systems, neural networks, and complex dynamic systems.

Jinliang Liu (Senior Member, IEEE) received the Ph.D. degree in control theory and control engineering from Donghua University, Shanghai, China, in 2011.

He was a Post-Doctoral Research Associate with the School of Automation, Southeast University, Nanjing, China, from December 2013 to June 2016. He was a Visiting Researcher/Scholar with the Department of Mechanical Engineering, University of Hong Kong, Hong Kong, from October 2016 to October 2017. He was a Visiting Scholar with the Department of Electrical Engineering, Yeungnam University, Gyeongsan, South Korea, from November 2017 to January 2018. He was an Associate Professor and then a Professor with Nanjing University of Finance and Economics, Nanjing, from June 2011 to May 2023. He joined Nanjing University of Information Science and Technology, Nanjing, in June 2023, where he is currently a Professor with the School of Computer Science. His research interests include networked control systems, complex dynamical networks, and time delay systems.

Engang Tian (Senior Member, IEEE) received the B.S. degree in mathematics from Shandong Normal University, Jinan, China, in 2002, the M.Sc. degree in operations research and cybernetics from Nanjing Normal University, Nanjing, China, in 2005, and the Ph.D. degree in control theory and control engineering from Donghua University, Shanghai, China, in 2008.

He is currently a Professor with the School of Optical-Electrical and Computer Engineering, University of Shanghai for Science and Technology, Shanghai. His research interests include networked control systems, cyber attacks, and nonlinear stochastic control and filtering.